Chapter 1

Introduction

The atmosphere that surrounds Earth is a complex and dynamic region of the planet. It comprises a multitude of phenomena that can be observed directly by humanity or the effects of which have an impact on life at ground level. Phenomena such as atmospheric gravity waves [*Vincent*, 1990], tidal activity [*Kato*, 1980], ion layers [*Mathews et al.*, 1993; *Mathews & Morton*, 1994] and aurorae [*Akasofu & Kamide*, 1987] are just some examples of the processes that are prevalent in the upper reaches of the atmosphere. At lower altitudes, the ever changing cloud formations and storm front activity are just two examples of dynamic atmospheric processes that are observed and experienced on a regular basis. These regions of the atmosphere are also intimately coupled (see e.g. *Hocking* [1996]). For instance pressure variations at ground level can seed gravity waves which break at much higher altitudes, transporting energy in the process.

Far from being an isolated system, the atmosphere also acts as an interface to extra terrestrial systems. For instance the Sun plays a major role in influencing the behaviour of processes within the atmosphere partly through the action of the solar wind. In a similar capacity the atmosphere is also an interface to interplanetary and interstellar space. Particles of various sizes occupying orbits within our solar system and beyond have been entering the Earth's atmosphere since it was formed. Typically, a large number of particles of the size order of sand grains, termed *meteoroids*, impact the

atmosphere as *meteors* and sometimes appear as shooting stars. This meteor activity typically takes place at altitudes of 70 to 160 km and injects their constituent atoms and molecules into the local atmosphere, ultimately adding to the Earth's total mass. Larger mass bodies, such as small asteroids or comets, have a much lower probability of impacting the atmosphere (e.g. *Brown et al.* [2002]), however their potential effects are more significant.

These larger sized masses, of diameter greater than about 10 m, when impacting our atmosphere down to ground level or detonating at some altitude above, are capable of devastating the established ecological systems with significant consequences for the continued existence of human kind. Even bodies smaller than this exhibit behaviour similar to nuclear detonations when terminating their travels in our upper atmosphere and thus can have an impact on international affairs if misidentified as such [*Tagliaferri et al.*, 1994]. Alternatively, rather than posing a potential threat to human existence, some authors theorise that these impacting bodies could be responsible for originating or contributing to life on this planet by the depositing of necessary chemicals (see e.g. *Bernstein et al.* [1999]). However, additional supporting evidence is required to validate these or other theories; if it is assumed that larger bodies have characteristics or properties generally similar to those of the smaller meteoroid complex [*Steel*, 1997; *Baggaley et al.*, 1994], then the study of these more frequent atmospheric impactors may provide the necessary answers.

In addition to the astronomical importance of the inherent properties of the meteoroid complex, a study of their ablation products as a tracer of processes in the atmospheric environment is nonetheless valuable. A primary example of this is the measurable effect upper atmospheric winds have on a forming meteor trail. This remote sensing of wind behaviour in the upper atmosphere is important in the pursuit of a comprehensive vertical wind profile for use in Global Circulation Models (GCM) as well as in investigations of specific local phenomena.

Radar (RAdio Detection And Ranging) is a powerful technique available to researchers to allow progress on many outstanding questions of meteor phenomena and

has been a powerful tool in atmospheric research since the 1920s. This is the technique applied in the work presented here. In particular, extensive use of a Medium Frequency (MF) Doppler radar located in the southern hemisphere is made in this study. The inherent operational characteristics of such a radar naturally lends itself to meteor observations due to its excellent coverage of the altitudes at which meteor activity appears, yet similar frequency radars have typically been under-utilised in this role.

This thesis describes research that was conducted into the MF Doppler radar system at Buckland Park near Adelaide. It includes ascertaining and solving equipment design and maintenance issues as well as the development of new hardware and the use of the optimised system to observe meteors.

Specifically, this chapter describes the context in which the present work resides, in terms of atmospheric and meteor science generally. Atmospheric nomenclature is described and the various meteor observational techniques available are briefly reviewed. The specific motivation and scope of this research is then delineated. Chapter 2 describes the equipment configuration and the techniques applied to establish a fully functional transmitting and receiving system. Chapter 3 discusses an investigation into the extensive antenna array network and provides an assessment of faults encountered, corrective work carried out and the development of techniques to ensure high operational levels are maintained in the future. Chapter 4 outlines the design, construction and evaluation of a new portable power combining system for the radar transmission system. Chapter 5 details the pertinent radar and meteor theory. Chapter 6 discusses the techniques applied to the data presented in Chapter 7. Conclusions and future work are then outlined in Chapter 8.

1.1 Atmospheric nomenclature

The scientific study of the atmosphere beginning in the first half of last century has led to the development of nomenclature to differentiate the different regions within

this environment [*Chapman*, 1950]. Several different classification schemes can be employed depending on the physical process being investigated. Commonly utilised classifications are based on thermal, chemical or constituent ionization and are illustrated in Figure 1.1. Thermal classification is based upon the typical temperature

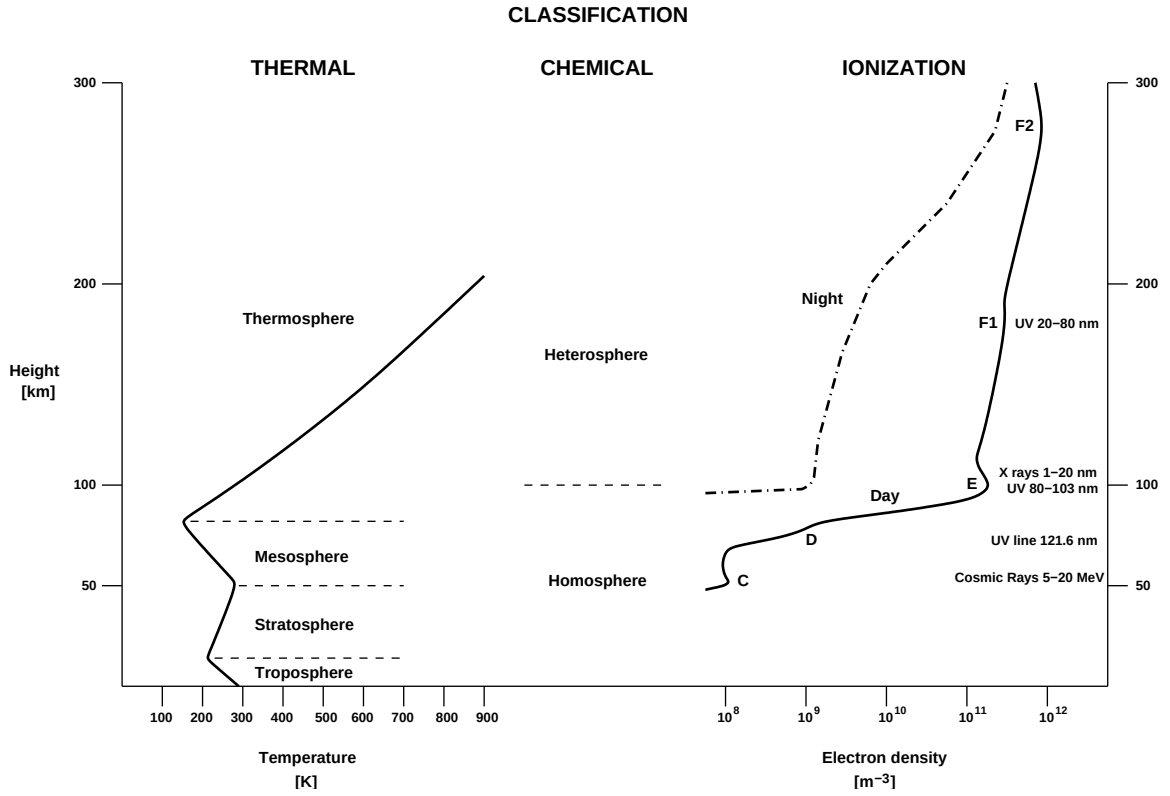

Figure 1.1: Atmospheric nomenclature. Illustrates three classification schemes applied to the atmosphere; Thermal, Chemical and Ionization. Sources of ionization for the distinct ionospheric layers are also indicated (adapted from *Hines et al.* [1965]; *Rishbeth* [1988]).

with altitude profiles of the atmosphere and identifies four distinct regions; the troposphere, stratosphere, mesosphere and thermosphere. The *troposphere* is characterised by a decrease in temperature from ground level to a height of approximately 10 to 20 km. The emission and absorption of infrared radiation by molecules such as water vapour, carbon dioxide and ozone provide efficient transfer of heat between different levels in this region [*Rishbeth & Garriott*, 1969] and manifest as a decrease in temperature with height that is partially offset by convection. From ∼20 to 50 km a steady increase in temperature defines the *stratosphere*. This temperature gradient is facilitated by the trace amount of ozone in this region. This stratospheric constituent

absorbs the ultraviolet (UV) solar radiation (<290 nm and partially 290 to 360 nm) and raises the temperature of the surrounding air. Above this altitude the temperature decreases again until a minimum ($\sim$180°K) is reached at approximately 80 km. The region enclosed between these two altitudes is termed the *mesosphere*. This temperature decrease occurs due to the decreasing Ozone density and the re-radiation of infrared radiation by CO_2. At altitudes above 80 km the temperature rises again due to the absorption of shorter UV wavelength radiation [*Roble*, 1987] and is termed the *thermosphere*. The altitudes at which a transition between temperature regimes occurs is indicated by the substitution of *-pause* for *-sphere* in the defined regions, i.e. tropopause, stratopause, mesopause. The stratosphere and mesosphere are often grouped together and termed the *middle atmosphere*, while *upper atmosphere* is similarly applied to the upper region of the mesosphere and thermosphere. It should be noted that the nominal altitudes defining the atmospheric regions vary with geographic location amongst other factors.

A chemical classification of the atmosphere centres around the behaviour of the atmospheric constituents (nitrogen, oxygen, water vapour, carbon dioxide etc.) in terms of their mean free path at varying altitudes. For altitudes below 100 km the constituent mean free path is small compared to that at higher altitudes and thus allows a high frequency of constituent collisions. This mechanism combined with the action of turbulence in this region results in the constituents being well mixed or homogeneously distributed and gives rise to the term *homosphere* to describe the chemical behaviour of this atmospheric region. Above 100 km constituent mean free path increases, decreasing the frequency of collisions. This factor, combined with the lack of turbulence at these altitudes allows constituents to behave relatively independently. This region is termed the *heterosphere*.

A third form of classification of the atmosphere particularly relevant to radio communication systems (including MF and High Frequency (HF) radar systems) is by constituent ionization. The *ionosphere* is defined as part of the upper atmosphere in which free electrons are sufficiently numerous to influence the propagation of radio

waves and extends from approximately 60 to 600 km in altitude [*Rishbeth*, 1988]. The stratified nature of this region was revealed by *Appleton & Barnett* [1925] and *Breit & Tuve* [1925] and later a nomenclature was ascribed to the dominant layers identified within this region. An increase in electron concentration of these layers with altitude is typical. The region below 60 km sometimes is host to a weak ionospheric layer termed the *C region*. This gives way to the more common *D region* at altitudes from 60 to 100 km. The *E region* occupies an altitude of 100 to 120 km. A maximum in electron concentration occurs between 200 and 300 km and this is the *F region* which encompasses the *F1* and *F2* local maxima. The dissociation and ionization of the atmospheric gases at these altitudes is caused by solar extreme ultraviolet (EUV) and X-rays. Because it is the solar radiation that produces the free electrons, the daytime ionosphere differs from the night time in its strength and number of constituent layers present and this is also illustrated in Figure 1.1. Interestingly, in the main layers of the ionosphere, less than 1% of the air is ionized and overall the ionosphere is electrically neutral to a high degree of approximation as positive and negative charged particles are always created and destroyed together yet a significant effect on radio wave propagation results from the small ionized component [*Rishbeth*, 1988].

1.2 Meteor phenomena and observational methods

A meteoroid has been defined by the International Astronomical Union (IAU) as a solid object moving in interplanetary space, of size considerably smaller than an asteroid but considerably larger than an atom [*Hughes*, 1993; *Babadzhanov*, 1993]. Below the lower mass limit of approximately 10^{-9} kg the term micrometeoroids is used and above the upper mass limit of about 10^{7} kg the term asteroid is more appropriate. The term *meteor* is applied to the luminous phenomenon that may arise, depending on size and velocity, as the meteoroid penetrates the atmosphere. Meteorites are the remnants obtained at ground level of a larger mass meteor event. Fireballs or bolides are meteoroids of sizes larger than 20 cm that impact the atmosphere [*Ceplecha et al.*,

1998].

As a meteoroid enters the atmosphere at high velocity the conversion of kinetic energy to other forms of energy facilitate its remote observations by various means [*Tagliaferri et al.*, 1994]. In approximate chronological order, techniques such as Visual; Spectral; Photographic; Radar; Photoelectric; Acoustic, Infrasonic and Seismic; Television and Video; and Satellite have been and continue to be used for this purpose. As is apparent by the development of approaches within this list, meteor observation techniques are closely linked with evolving technologies.

The majority of these techniques are *passive*, where energy from the meteor event is radiated to the particular detector directly and pertinent information extracted. In contrast to this the radio or radar technique is an *active* technique characterised by a transmitter acting as a primary energy source directing radiation toward the meteor event with a receiver detecting the small fraction of radiation returned. This approach has some distinct advantages in comparison to the traditional passive approaches. Each technique has its inherent capabilities and the following paragraphs outline the various techniques and touch upon their inherent advantages and disadvantages.

Visual observations of meteors utilise the unaided or aided naked-eye in observations of opportunity or coordinated campaigns. Such observations of meteors have been applied in various forms throughout a large part of human history [*Fedynsky*, 1959; *McKinley*, 1961; *Hawkins*, 1964], primarily because the behaviour of the heavens assumed significant importance in many cultures. These early visual observations reveal little in the way of useful scientific data save for the valuable occurrence record of meteor events throughout the centuries. One parameter often recorded in later visual observations is the *magnitude*. This refers to the brightness of a celestial object on a scale where an increasing magnitude value indicates decreasing intensity. The term *apparent magnitude* refers to the brightness of the object as observed from Earth and is a combination of intrinsic brightness and the dimming due to the object's distance

from the point of observation[1]. For instance the apparent magnitude of the Full Moon is -12.6 and that of Venus is approximately -4, depending on its orbital position. Unaided visual observations have the potential to detect meteors to an order of $+5$ to $+6$ magnitude and overwhelmingly occur during the night. From a single observation point meteor trajectories may be plotted on a star map and parameters such as radiant position[2], hourly rate, magnitude distributions and rough estimates of meteor speed may be deduced.

McKinley [1961] identifies the work of *Brandes* and *Benzenburg* at the start of the nineteenth century as the founders of modern visual observing techniques by their observations of the same sky region from two ground locations that ascertained the the height of meteor events to occur at about sixty miles above ground level and to have velocities high enough to have originated from outside the Earth. Observations employing binoculars or small telescopes allow events of magnitude down to about $+12$ to be detected although the limited field of view of this equipment doesn't enable any significant increase in the number of meteors observed in comparison to unaided visual methods. A further advance in the measurement of meteor speeds was initiated by *Öpik* [1934] via observing the meteor through a rocking mirror and deducing the meteor angular speed using the number of whorls in the trail. Techniques applied to the visual observation of meteors have been steadily improved over the ensuing years and a systematic approach is encouraged by the many amateur meteor organizations such as the International Meteor Organization (IMO), American Meteor Society (AMS), Nippon Meteor Society (NMS), Dutch Meteor Society (DMS) among others.

Benefits of the visual observation of meteors are that the unaided eye can detect meteors fainter than some small cameras and that visually derived magnitude relations are often referred to by photographic and radio studies. In addition, meteor observations have been historically recorded via visual techniques and thus establishing the

[1] *Absolute magnitude*, in general, describes the magnitude of the celestial object if placed at a distance of 10 parsecs from the Sun. If used to describe the brightness of a meteor this usually refers to the magnitude it would have if it were placed in the zenith at a standard height of 100 km.

[2] Defined as an area in the sky from where the shower meteors appear to emerge and traditionally named after the nearest constellation.

relation between these observations and current alternative observational techniques allows present results to be placed in the proper context [*Ceplecha et al.*, 1998]. Primary disadvantages of this observational technique are the limited accuracy of derived parameters; the lack of permanent record of meteor event for later re-interpretation; the dependence on favourable or ideal atmospheric observing conditions; limited field of view of binoculars and telescopes; the significant time and human resource required and the scientific analysis of the accumulated data is often limited to a statistical interpretation only.

Meteor spectral observations were first carried out in the later 1800's as an extension to visual observation techniques where a binocular prism spectroscope was used to view a meteor event as it occurred [*McKinley*, 1961; *Ceplecha et al.*, 1998]. This technique reveals the emission lines and thus chemical composition of the meteor and less significantly of the atmosphere [*Kresák & Millman*, 1968]. Diffraction gratings were later used to disperse the light and obtain similar results [*Kresák & Millman*, 1968]. The transient nature of this approach was aided by recording the spectrum on various mediums. This began with the use of photographic plates in 1897, which has remained a primary spectral recording medium. Relatively recent uses of television in meteor spectroscopy (since 1969) [*Ceplecha et al.*, 1998] first utilised motion picture cameras for permanent record, with later developments allowing hard copy of the video image and now image digitization. Later spectral photographic techniques provide a better resolved spectrum for analysis: however television techniques have the advantage of allowing a time and spatial evolution of the spectra.

Photographic techniques have been applied to capturing meteor phenomena since *Weinek* photographed a meteor in 1885 above Prague [*Ceplecha et al.*, 1998]. Documenting meteors of opportunity via this technique occur to the present times, however valuable scientific data is more often gleaned from dedicated photographic meteor observations programmes. Various techniques may be applied using single or dual camera arrangements [*McKinley*, 1961; *Katasev*, 1964]. However a popular method (mirroring that of the more advanced visual technique) utilises two cameras separated

by a distance of some 20 to 50 km with some observational area overlap at typical meteor heights [*McKinley*, 1961]. If a rotating shutter is employed on one or both of the cameras the angular velocity of the meteor may be attained and a linear velocity deduced if the position and orientation of the path is determined. It is also possible to estimate meteor deceleration due to air resistance with this method and derive preliminary estimates of upper air density [*Hawkins*, 1964]. Studies utilising equipment similar to this have been made by Elkin (1893 to 1909) [*Elkin*, 1900] and Whipple (1936 to 1942) [*Whipple*, 1938; *Whipple*, 1954]. The small cameras used for photographic investigations are limited to meteors with an apparent brightness of 0 to -1. To register meteors to $+4$ magnitude but retain a large field of view, the Super-Schmidt cameras were developed specifically for meteor work during the early fifties (camera designed by Schmidt and modified at Harvard by Baker, see *McKinley* [1961]; *Hawkins* [1964]).

Advantages of the photographic technique are that a permanent record of the event is obtained which can be re-examined at a future date, given any additional information or renewed purpose. Also the photographic records are significantly more accurate than visual records. Disadvantages of meteor photography are that it is not a complete substitute for visual observations due to the limited magnitude capabilities of some cameras, and that single camera systems generally cover a limited portion of the sky which results in a low hourly meteor count rate. As with visual techniques, the photographic technique relies on favourable atmospheric conditions which may preclude its extended use at many sites.

As discussed previously, the radar technique is an *active* observational technique where electromagnetic radiation is directed toward the meteor event and the radiation reflected is detected at a receiver. A typical sand-grain sized meteoroid itself impinging on the earth's upper atmosphere will reflect a negligible amount of radiation in most radar systems. However the summation of echoes from the ionized trail produced by the ablating meteoroid will result in a significant signal detected at the receiver and it is this signal which is examined for characteristic meteor parameters and parameters

of the surrounding environment.

Initially, radar systems used for other purposes were applied to meteor observations. This practice later gave way to purpose built equipment with single and multiple station backscatter radars arrangements being the primary configurations as well as the limited use of forward scatter systems[3]. These radars have operated in continuous wave (CW) or pulsed mode and have employed frequencies from MF to Ultra High Frequency (UHF) (e.g. *Pellinen-Wannberg & Wannberg* [1994]; *Zhou et al.* [1995]; *Mathews et al.* [1997]). Recently, digital ionosondes have been used for meteor observations (e.g. *Berkey & Fish* [2000]; *MacDougall & Li* [2001]). In concert with the radar hardware development over the ensuing years, techniques have evolved for meteor parameter measurement from the acquired meteor echoes. Parameters such as echo rate, height, decay and duration time, speed or velocity, upper atmospheric wind, diffusion coefficient etc. have been routinely derived from these observations while meteor orbits have been ascertained from multi-station observations.

The first accurate identification of the mechanism by which meteors are detected by radar is attributed to *Skellett* [*Skellett*, 1931; *Skellett*, 1935] and *Schafer & Goodall* [1932]. Various investigations were conducted up until World War II, but it wasn't until the rapid development of radar systems with carrier frequencies higher than the E and F region critical frequencies that radar meteor research gained momentum. Principal advantages of radar observations are the ability to detect meteors to an equivalent magnitude of approximately +15[4] depending on the radar system's specific capabilities and the ability to observe meteors continuously during day and night (mid HF and Very High Frequency (VHF)) or night time (MF and low HF). Weather does not affect the radar's operation and most radar systems can operate autonomously for extended periods. A notable disadvantage is the initial expense of the chosen radar

[3]If the receiver is located near the transmitter, the system is described as a *backscatter* radar whereas if the receiver is separated from the transmitter by a distance similar to, or greater than, the distance of the target from either station, then the system is a *forward scatter* radar [*McKinley*, 1961].

[4]The capabilities of a radar system can be related to visual magnitude by the experimentally derived radio magnitude relation $M_v = 36 - 2.5\,(\,log_{10}\,q - log_{10}\,V\,)$ [*McKinley*, 1961], where q is the electron line density of the trail (e/m), and V is the meteoroid speed (km s^{-1}).

system. Also different frequencies exhibit biases towards specific height ranges.

One technique briefly investigated by researchers in Canada [*McKinley & McKinley*, 1951] and Russia [*Astavin-Razumin*, 1958] was that of photoelectric meteor observations employing a system of photomultiplier tubes. Meteors brighter than +3 could be detected in certain circumstances with this type of technique. If an array of photomultiplier tubes was used to cover the sky, an approximate meteor position could be obtained as well as an estimate of light intensity. Providing the meteor event excited multiple detectors, a raw estimate of meteor direction could also be obtained. A specific advantage of this type of technique was the precision timing of the meteor event which could be best capitalised on when used in conjunction with radar or visual observing techniques. Disadvantages were the photomultiplier tubes susceptibility to sky noise produced from star scintillations and random light sources as well as the small field of view of each individual detector, thus necessitating the implementation of some form of array. *McKinley* [1961] suggested this technique had potential for improvement (later re-applied by *Cook et al.* [1980]) but it has effectively been superseded by television techniques.

First applied in the 1960's, television observations of meteors continues to the present day in various forms (e.g. *Jones & Sarma* [1979]). Earlier observations were conducted with unintensified image cameras but later devices included image intensifiers coupled to the camera, providing optical gain, and are termed low-light-level television (LLLTV) systems. The resulting signal was often recorded to tape with progress to video digitization occurring relatively recently. Meteors down to an apparent limiting magnitude of +9 can be observed with these systems. Single station systems typically observe mass index and mass flux, while dual stations allow meteor trajectory via triangulation. Meteor orbits and populations as well as spectra can also be derived with some systems [*Hawkes & Jones*, 1986].

The television technique can rival radar techniques in trajectory accuracy and is less biased against high altitude meteors. Disadvantages are that the field of view is often small and atmospheric conditions again play a role in the signal to noise ratio

obtained for faint meteors. Although the detection process in television systems is more straightforward than radar, the subsequent data analysis of an event is time consuming and complex even with the advance frame grabbing and digital image processing software.

The meteor observation techniques described in the preceding paragraphs are all ground-based systems. The proliferation of satellite platforms over the last three decades offers an alternate view of meteor activity and the application of different types of sensors. The application of satellite platforms to meteor observations has been discussed by *Tagliaferri et al.* [1994]. Many satellites currently have downward looking infrared, visible and ultraviolet light sensors while some are outfitted with radar capabilities. Some Department of Defense (DoD) satellites are equipped with transient radiometric sensors that can record the visible light flashes produced by nuclear detonations, intercontinental ballistic missile ignitions, lightning and bright meteors. This sensor typically has a near hemispherical field of view (at typical satellite altitude of 20,000 km) with a single silicon photodiode and is able to measure the relatively low light intensity of meteoroids impacting the earth's upper atmosphere. With digital signal processing and the input from other satellite systems the position and other parameters can be determined for these events. To date, only bright meteors have been reported with these systems, partly as a direct consequence of the system being optimised for non-meteor events. However, upgrades to the global positioning system (GPS) satellites include these sensor systems and may offer a significant opportunity for meteor studies to be undertaken. A more fundamental spaceborne detector is that of the spacecraft itself. Meteoroid impacts on the various structures of satellites have been measured to provide mass distributions and compositional information [*Laurance & Brownlee*, 1986; *Love & Brownlee*, 1993].

Advantages of the satellite system are of course the dramatic increase in region covered and the omission of dense atmosphere between sensor and meteor event. With a relatively small number of satellites, continual coverage could be provided. Disadvantages are the expense of multi-function satellite platforms and the small set of

successful meteor detections reported to date. Also, if spacecraft impact data are required, physical retrieval of the component is necessary for analysis.

Other observational techniques include acoustic, infrasonic and seismic observations [*Ceplecha et al.*, 1998], however these have been typically only applied to bolides and distinctly brighter meteors. Spacecraft missions to meteoroid sources such as asteroids and comets [*Keller et al.*, 1986; *Langevin et al.*, 1987; *Thomas, Kramm & Keller*, 1988; *Gehrels*, 1994] is a significantly advanced technique to deduce meteor information but will not be discussed further here.

The advantages of the radar observational technique has seen it employed on a wide scale and become established as a primary source of data on meteor phenomena. The research presented in the following chapters has used a MF radar operated during the late evening and early morning (pre-sunrise) hours for meteor observations.

1.3 Motivation and scope of thesis

Prior to the undertaking of meteor observations that utilised the MF Doppler radar, a lightning strike to the antenna array resulted in significant equipment damage. To allow a re-establishment of routine observations from the site, this specific damage was repaired. During this initial repair period, more thorough investigations into the complete radar system, comprising the transmitter, receiver and antenna array, indicated some hitherto unknown system deficiencies. These deficiencies had a direct bearing on the systems ability to undertake more demanding experimental observations proposed, such as the investigations of meteor activity described in this thesis. Because of this situation, efforts were directed to the isolation and repair of all discernible system faults. It is of prime importance that equipment performance is to specification if valid judgements are to be made from the data collected. This was the primary motivation of the research conducted into system behaviour. Secondarily, continued, full time operation of a radar system requires regular preventative maintenance to ensure maximum time is devoted to routine observations. This is never more vital than in a

system with ageing components. To facilitate this, effort was devoted to establishing tests that monitor the performance of core system components and developing maintenance procedures to correct commonly encountered problems. This work is described in Chapters 2 and 3.

The first of these chapters details the problems encountered within the transmitter and receiving system and outlines the possible solutions and those implemented. Because of the often common design exhibited in individual Doppler radars, the approaches used here are applicable to other similar systems. The second of these chapters details an investigation into the 1 km diameter antenna array. As a core component of the complete radar system, its performance is of importance to the overall quality of data obtained. The physical size and age of this antenna array provides for a variety of ailments and dictates that a methodical approach to fault investigation is warranted. The extensive cable system was evaluated primarily using time domain reflectometry techniques with specific methods developed to maintain a high level of operational capacity post maintenance. Statistical data on the occurrence of typical faults was also required for future estimates of array serviceability.

As a highly modular system, the core radar hardware offers opportunity for expansion of its capabilities via the addition and integration of additional hardware. Changing experimental demands required a non-standard configuration of the power modules within the transmission component of the radar system. This motivated the design and construction of a portable power combining system to achieve the experimental requirements. This resulting system and its genesis is described in Chapter 4.

The now fully operational MF radar could then be applied to current problems in meteor science. Previous studies [*Olsson-Steel & Elford*, 1987; *Elford & Olsson-Steel*, 1988] have shown radars at low frequencies (MF and low HF) to be capable of extending the observed heights of meteors in comparison with standard VHF meteor radars. This is due to the height ceiling increasing as radar carrier frequency lowers. Mean meteor heights are about 10 km higher in the lower frequency studies than the approximate 95 km height of VHF studies. Thus true meteor height distributions

cannot be obtained from VHF observations alone and a more accurate representation is only possible with the inclusion of lower frequency radar data. In fact it has been suggested [*Steel & Elford*, 1991] that 50% of all meteors trails above 105 km remain undetected and more research in this area has been called for [*Elford*, 2001*a*].

In this respect MF radar observations of meteors offer a different perspective on the meteoroid complex. The study outlined in the remaining chapters of this thesis concerns meteor observations at this frequency with a particular focus on observations conducted on the Orionids peak activity night of 22 October 2000. The meteor echoes observed were analysed using a coordinate transform technique developed by *Elford* [1954] whereby meteor reflection point data is transformed to a celestial reference frame. This allows "linear associations" of meteors to be isolated in the data corresponding to particular shower radiants. This selected meteor component is then examined in terms of other meteor echo parameters.

Vital to a study of this type is the determination of meteor speeds. Traditional meteor speed techniques applicable to VHF meteor events may not be appropriate to those echoes recorded at MF due to the low radar PRFs used and because of the variable ionospheric environment obscuring echoes. *Cervera* [1996] proposes that the pre-t_0 technique (see sections 5.2.2 & 5.3.1.3) may be applicable at these frequencies and this suggestion is also evaluated.

Chapter 2

Equipment

The data presented in the following chapters were acquired using the 1.98 MHz (MF) Doppler radar located at the Buckland Park Research Facility, Adelaide, Australia. This radar and other atmospheric sensors at the site provide comprehensive coverage of the middle atmosphere and components of the upper atmosphere. The specific height coverage of these sensors is detailed as is their physical location within the Buckland Park site.

In terms of system arrangement, the MF Doppler radar has some noticable differences from many beam steering atmospheric Doppler radars. Its distributed modular design and 1 km wide antenna aperture serve to distinguish it from similar frequency radar systems. This antenna array is first described followed by an overview of the transmitting and receiving hardware. The fundamental operation of a pulsed Doppler radar is then depicted with an emphasis on those components and modes of operation of this particular radar pertinent to later discussions.

An evaluation of the radar system in general was undertaken in order to address some concerns with recent radar performance and the uncovered system faults are described as well as the solutions implemented. This fault rectification process facilitated the selection of any desired phase shift in beam forming and optimised transmitted power such that a previously untried configuration for meteor detection and analysis at the Buckland Park site could be implemented. The need for the development of

new radar hardware, such as a power combining system, is then touched upon with a full discussion appearing in Chapter 4. Directions for future work in terms of the radar transmit and receive systems are then outlined.

2.1 The Buckland Park research facility

The Buckland Park research facility is the primary field site for the middle and upper atmospheric research conducted by the Atmospheric Physics Group of the Department of Physics, University of Adelaide. This site (35° 38′S, 138° 28′E) is located on a flat coastal plain 3.25 km from the Gulf St. Vincent and approximately 40 km from the city centre of Adelaide in South Australia. Aside from the immediately adjacent expanse of water and peninsula, the surrounding topography consists of a gradual rise of surface elevation from approximately sea level, through the Adelaide Plains and culminates in the Mount Lofty Ranges situated approximately 48 km from the site at an elevation of over 700 m. The local geographic area is part of the environment in which the radar operates and as such can have a partial influence on the radar signal received. In this regard the local geography may contribute to the generation of atmospheric disturbances that give rise to radar echoes from the middle atmosphere. For instance gravity waves can be generated by the passage of cold fronts over the local topography [*Ball*, 1981] and then propagate through the radar beam at mesospheric heights. Alternatively, as the range gates of the radar extend over 100 km, echoes from the distant mountain ranges, surface features [*Grant*, 1995] or sea-surface [*Vandepeer*, 1993] may contaminate the data due to the broad radiation pattern of the MF array dipole antennas. Once a relatively isolated site, the encroachment of residential housing and the development of agricultural techniques for use on existing farming areas (e.g. irrigation pumps) sees the site subjected to increasing levels of human-made Radio Frequency (RF) interference, but this has not yet significantly affected routine radar operations. Aside from these factors it is a typical mid-latitude site with geomagnetic field of intensity 5.9 $\times 10^{-5}$ Wb m^{-2} and a dip angle of 67° [*Elford & Taylor*,

1997].

Atmospheric research has been conducted from the site since the late 1960's utilising various techniques and equipment. It continues to the present time with a dual focus on research into new atmospheric observing techniques and maintaining established atmospheric observations. Buckland Park routine atmospheric observations are well suited for comparison with radar data from other sites and for input into global circulation models.

This research site houses a number of types of remote sensing equipment that provide information on atmospheric dynamics in the region from ground level to heights exceeding 100 km. Currently four radars operate from the site. The 1.98 MHz MF Doppler radar [*Reid et al.*, 1995] for routine observations from 50 to 100 km and the development of new research techniques. A newly commissioned 31.0 MHz Meteor Detection Radar (MDR) complete with two crossed dipoles for transmission and a crossed interferometer arrangement of five dipoles for reception, obtains meteor echoes in the 70 to 110 km height region [*Holdsworth & Reid*, 2002]. A 54.1 MHz VHF ST (Stratosphere-Troposphere) limited beam steering Doppler radar [*Vincent et al.*, 1987; *Hobbs*, 1998] which currently alternates its mode of operation between atmosphere wind measurement (2 to 15 km) and meteor detection and analysis (70 to 110 km). The 54.1 MHz VHF Boundary Layer (BL) radar [*Vincent et al.*, 1998] for sensing the lower region of the troposphere over a height range of 400 to 3200 m is used in alternation with the previously mentioned radar occupying this frequency. A Radio Acoustic Sounding System (RASS) can operate in conjunction with either of the 54.1 MHz radars in order to obtain temperature profiles in the troposphere over heights from 400 to 2000 m.

Various night time optical instruments are also operated from BP due to its relatively isolated location from extraneous light sources. The Three Field Photometer (TFP) is located in the transportable laboratory at the centre of the MF array and observes airglow emissions of the OH (6-2) band and OI line (using 730 and 557.7 nm filters) generated at heights of approximately 87 and 94 km respectively [*Hecht et al.*,

1997; *Woithe*, 2000*a*]. An Aerospace Airglow Imager (AAI) [*Hecht et al.*, 1994] of the Space and Environment Technology Center is also operated from this location to observe the OH Meinel (6,2) band and the O_2 atmospheric (0,1) band nightglow which cover height ranges 85 to 90 km and 90 to 95 km respectively, using a number of different wavelength filters. A CCD Spectrometer (CCDS) (e.g. *Sivjee et al.* [1999]) of Embry-Riddle Aeronautical University records airglow emissions in the region 760 to 900 nm and derives temperatures from a range of OH airglow bands encompassing an approximate height range of 85 to 95 km. This device is located in a transportable laboratory near the south-east corner of the field site. An Automatic Weather Station (AWS) [*Davis Instruments*, 1996] also provides measurement of pressure, humidity, temperature, dew-point, rainfall as well as wind speed and direction at surface level. The relative locations of the individual sensors at the Buckland Park research facility is displayed in Figure 2.1 and their height coverage is summarised in Figure 2.2.

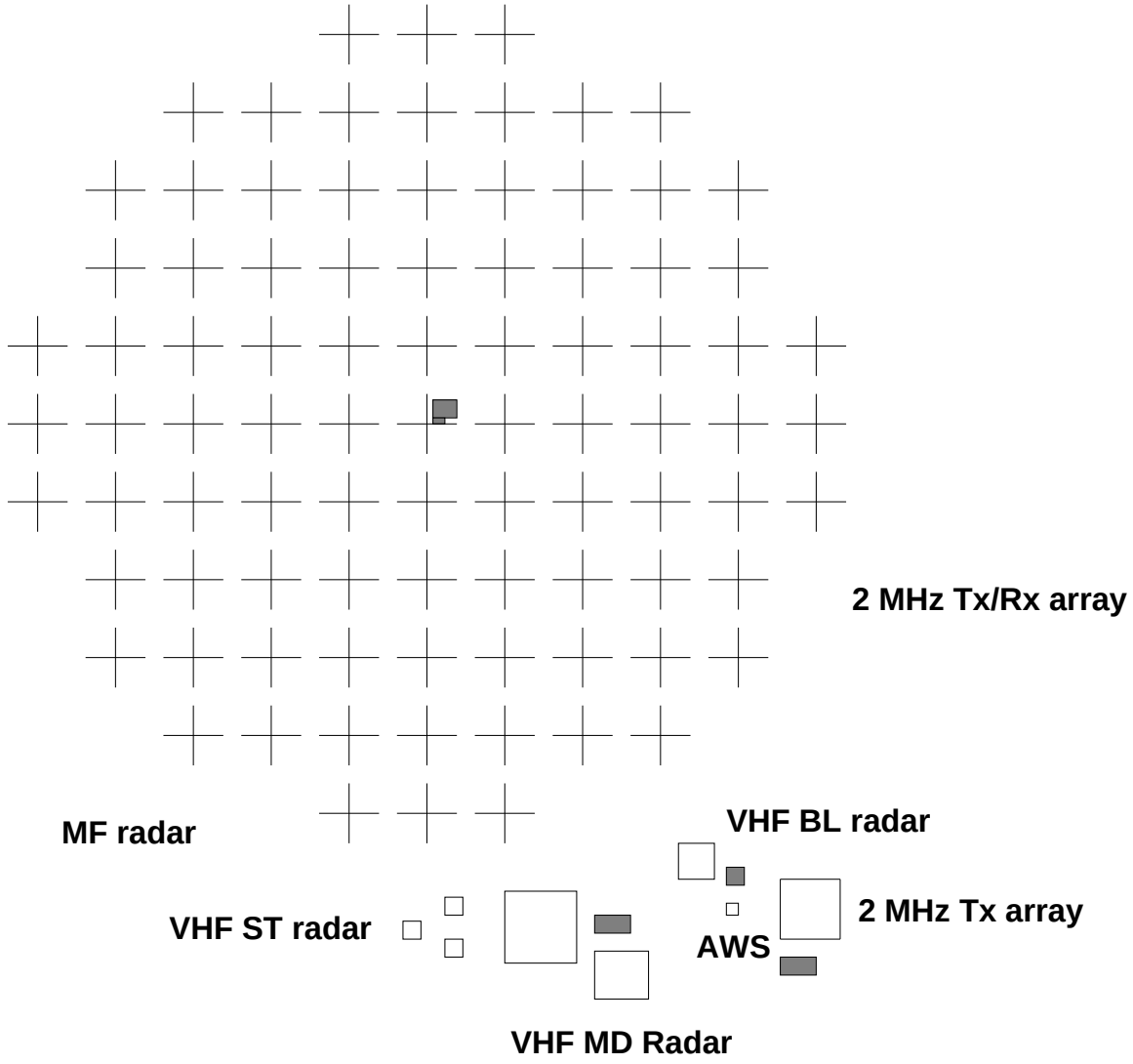

Figure 2.1: Location of the primary atmospheric sensors at the Buckland Park research facility. Infrastructure, such as the main transportable laboratory located at the centre of the MF antenna array, is indicated by the shaded areas. The main laboratory also houses two of the three optical instruments. Adjacent to the main laboratory is the cable phasing room that maintains the multiple half wavelength cable sections to each antenna.

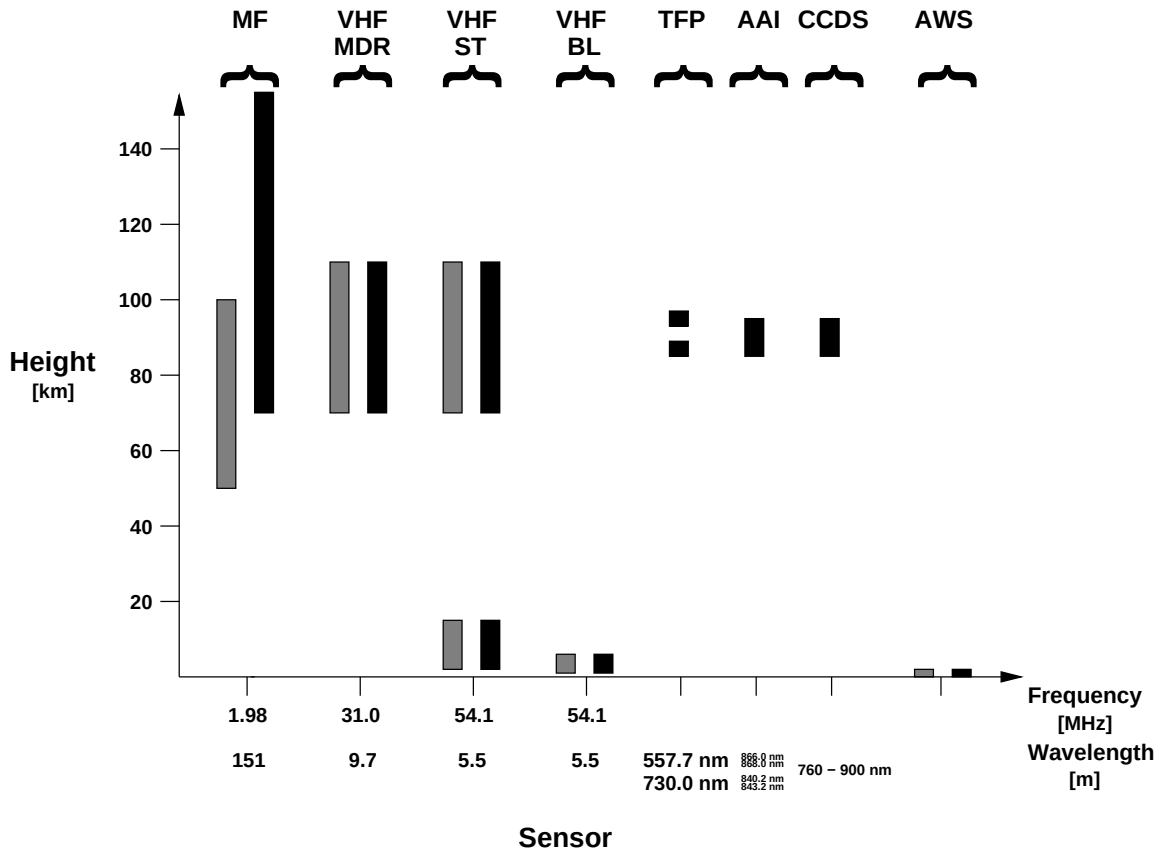

Figure 2.2: Height coverage of the primary sensors at the Buckland Park research facility. The day (grey) and night (black) time coverage is indicated. The frequency and wavelength of the respective sensor, where applicable, is indicated on the abscissa.

2.2 The Buckland Park MF Doppler radar

The Buckland Park MF radar system was conceived in the 1960's primarily to study the diffraction pattern produced by radio wave scattering from the ionosphere [*Briggs & Elford*, 1968] and it is for this task that determined a great deal of the radar's hardware arrangement still in use today. As the main ∼1 km diameter antenna array was initially used for reception only, in a bistatic configuration with transmission from a nearby but separate array, its design parameters were optimized accordingly. Prior to the construction of this array, antenna configurations employed to sample the ground diffraction pattern mostly utilised the hardware of three receiving antennas and employed the so-called Spaced Antenna (SA) technique (e.g. *Mitra* [1949]; *Briggs et al.* [1950]; *Briggs* [1968]). However, this method made assumptions inconsistent with observation that could possibly be resolved using an array large enough to sample two or three maxima and minima of the ground diffraction pattern [*Briggs et al.*, 1969]. This required individual antennas to be separated by no more that 100 m and thus established the arrays basic form. Subsequent research using this antenna array has resolved many of the concerns with this technique and has contributed to the development of the Full Correlation Analysis (FCA) technique (e.g. *Briggs* [1984]) now commonly used to estimate atmospheric winds.

Another important feature of the antenna array is the arrangement of phasing cables connecting individual antennas to the radar hardware, whose lengths are designed to reproduce the amplitude and phase of the voltage recorded at the dipole at the receivers. This established the distinctive layout of cable that is the MF antenna array (see *Rossiter* [1970] or Figure 3.24 in Chapter 3). The interface between these individual antenna cables and the transmitting and receiving radar hardware is also of note. A high degree of flexibility in choosing individual or groups of antennas has been incorporated into the system design philosophy. This is often in contrast to other atmospheric or Mesosphere-Stratosphere-Troposphere (MST) radar systems that provide a fixed transmission and reception antenna configuration for specific-purpose

atmospheric sensing. These factors have enabled the system to be applied to research in the areas from meteor physics to radio astronomy (e.g. *Briggs et al.* [1969]; *Briggs et al.* [1972]; *Briggs* [1993]; *Hocking* [1997*a*]).

2.2.1 Description of the MF Doppler radar antenna array

The antenna array comprises 89 crossed half-wavelength dipoles arranged on the nodes of a rectangular 11×11 grid. The complete arrangement forms a roughly circular aperture of 914 m diameter. It can be used for transmission and reception. The array was originally oriented to be parallel with the road on the eastern boundary of the site and as such lies 3°46′ west of True North (TN) [*Department of Lands*, 1976]. The array was designed to operate at a frequency of 1.98 MHz with the facility to receive at its third harmonic of 5.94 MHz. To obtain a near symmetrical beam pattern and accurate pointing direction from a large diameter aperture the site needs to be topographically quite flat. *Reid* [1984] found that the mean surface gradient under the array is less than 0.10° and that a nominally vertically pointing beam is about 0.1° from the zenith at an azimuth angle of about 225°.

Each centre-fed dipole element is a nominal 71.6 m in length comprising two 35.8 m lengths of hard-drawn copper wire, 2 mm in diameter. Each crossed dipole pair is mounted at its centre feed point on a wooden pole support nominally 10 m above ground level. Adjacent crossed dipoles are positioned at 0.60λ (91.4 m). To maintain consistent dipole elevation above ground and minimize the number of overall support posts each dipole is connected to the adjacent dipole (or outer support post) via a 19.8 m section of insulator.

The dipoles in each pair are orthogonally mounted with one aligned approximately north-south and the other east-west. An individual dipole exhibits a nominal impedance of 28 Ω at the transmit frequency of 1.98 MHz and is matched to its coaxial feed line by a balun for operation at 1.98 MHz. This balun incorporates a relay which can switch the balun transformation provided to 97 Ω for a dipole at 5.94 MHz via a DC voltage applied by the radar Filter/Transmit-Receive (Filter/TR) switch module

through the coaxial cable feeder.

The balun unit comprises a circuit for each orthogonally mounted dipole. This arrangement results in two separate coaxial cable systems routed back to the antenna patchboards at the main laboratory for the respective dipole. To preserve the transmitted phase on each multiple half wavelength cable, a 180° phase shift is introduced at the dipole by reversing the balun connection feeds. The coaxial cable system for each single cable feed comprises two similar cable types, the original 70/75 Ω air-cored Aeraxial coaxial cable and a smaller section of recently installed solid-cored 75 Ω Belden 8213 RG-11/U coaxial cable. The total cable system length approximates a multiple half wavelength so as to reproduce the voltage detected at the dipole at the patchboard input. The Belden 8213 RG-11/U is routed in plastic conduit down the ten metre support pole and joins the lengthy underground section of Aeraxial cable which is then routed through the cable phasing room located adjacent to the main radar laboratory (see *Rossiter* [1970, Figure 3.5]) and then into the main laboratory where it terminates at either of the two polarisation antenna patchboards.

The antennas can be used individually or in groups for transmission or reception duties, providing the peak voltage of the balun is not exceeded in any configuration. Design studies [*Vandepeer*, 1993] indicated that an optimisation of the current transmitting and receiving hardware (in terms of cost versus performance) utilised one group of three dipoles connected to the single Filter/TR switch module of each channel, with as many channels configured as needed for transmission and reception. This is the configuration used for most applications.

The antenna patching arrangement is facilitated by three patching boards located adjacent to the transmitting equipment contained in the main laboratory. Two antenna patchboards, accounting for the two antenna polarisations, facilitate the connection of individual antennas into dipole groups and a third (centre) patchboard routes these selected groups to the transmitter/receiver system. Of the two antenna patchboards, one patchboard houses connection points for the 89 north-south dipoles and is labelled the *East* polarisation patchboard as each dipole's radiation maximises

in an easterly direction while the other patchboard in labelled *North* (a photograph showing the *East* antenna patchboard is displayed in Figure 3.1 (page 101) of Chapter 3). Groups of antennas then connect to a transmitter channel via the centre transmitter patchboard which provides a match for the three 75 Ω dipole feeds to the nominal 25 Ω of the transmitter channel I/O. The length of all patching cables used in dipole selection and routing to individual Filter/TR switch modules is minimised so as to limit introduced phase discrepancies. Typical impedance values presented to the transmitter Filter/TR switch module by ten groups of three antennas are displayed in Table 2.1. This table shows a relatively close match to the Filter/TR switch module

Tx Channel	$\lvert\mathbf{Z}\rvert$ [Ω]	$\angle\mathbf{Z}$ [°]
1	24.1	−1·5
2	24.3	7·4
3	23.5	10·0
4	27.5	−6·1
5	26.0	7·6
6	24.8	7·9
7	24.4	7·9
8	28.1	4·8
9	26.9	8·3
10	24.0	10·7

Table 2.1: Typical impedance values of ten antenna groups measured at the Filter/TR switch module I/O. Each group impedance value is a function of the three connected dipole impedances. The expected nominal impedance value is 25 Ω ∠0°. Variations of ±5 Ω and ±15° are considered normal under varying local environmental conditions.

I/O, providing near optimum power transfer from transmitter module to antenna and a low VSWR.

The radar was operated in bistatic mode for many years. In this mode of operation transmission was achieved by a small antenna array located adjacent to the then, reception only, main MF array. This transmission array comprised two sets of parallel dipoles in a square arrangement to achieve linear or circularly polarised radiation. This array is described in *Murphy* [1990] and *Vandepeer* [1993] and although not used in this current work can be accessed via underground cable feeds within the MF radar

laboratory for specific experiments if desired. As circular polarisation on transmission has only been tested on the main array to date, this original transmission array still has some application (see Chapter 4).

Currently all transmission and reception duties are carried out utilising dipoles within the main array. A standard configuration of dipoles for transmission was employed for the meteor mode observations in order to facilitate a seemless transition to alterate radar modes (i.e. FCA, Differential Absorption Electron (DAE) concentration measurements, etc.) at the completion of the scheduled meteor observation period. This configuration comprised twenty-six groups of three dipoles from the *east* patchboard arranged to optimise the final vertically transmitted beam width and is displayed in Figure 2.3. In this figure each antenna group is ascribed a transmit channel number. The maintenance conducted on the antenna array as described in Chapter 3 allowed a significant increase in the number of dipole systems available for this configuration.

The transmitted beam has been modelled previously for the original array [*Olsson-Steel & Elford*, 1987] and the current upgraded array [*Vandepeer*, 1993; *Holdsworth*, 1995] using various array layouts based on the standard equations for the radiation pattern of a single dipole element (e.g. *Jasik* [1961]; *Krauss* [1988]).

The modelling of the fields produced by electric and magnetic sources is a constantly evolving field and over the last two decades has incorporated the detailed numerical results offered by the exploitation of digital computers, ultimately giving rise to the discipline of Computational Electromagnetics (CEM). Within this sphere of study various approaches to the modelling of Electromagnetic (EM) sources may be taken and a comprehensive review of these is detailed in *Miller* [1988]. Essentially, the numerical methods can be divided into integral or differential equation based techniques with the notable techniques in each respective class being the method of moments (MoM) and the finite difference time-domain (FD-TD) method [*Stutzman & Thiele*, 1998]. The MoM is a well established technique and is the basis of the software

application Numerical Electromagnetics Code - Version 2 (NEC-2) [*Burke & Poggio*, 1981] used in this instance.

The modelling results for a vertically directed beam based on the physical antenna layout displayed in Figure 2.3 is illustrated in Figure 2.4. The half power full width is ∼10° and the dominant sidelobe structure occurs at 15° off-zenith and is 16 dB down on the main lobe power.

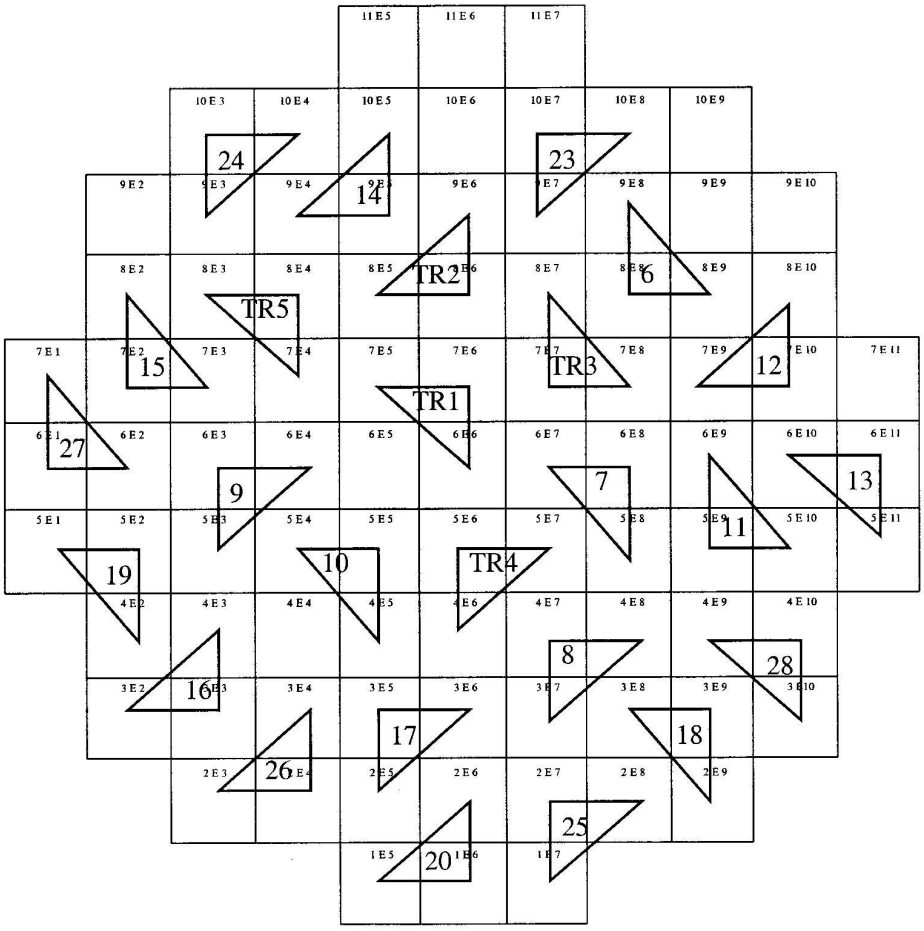

Figure 2.3: Transmission antenna configuration for meteor experiments.

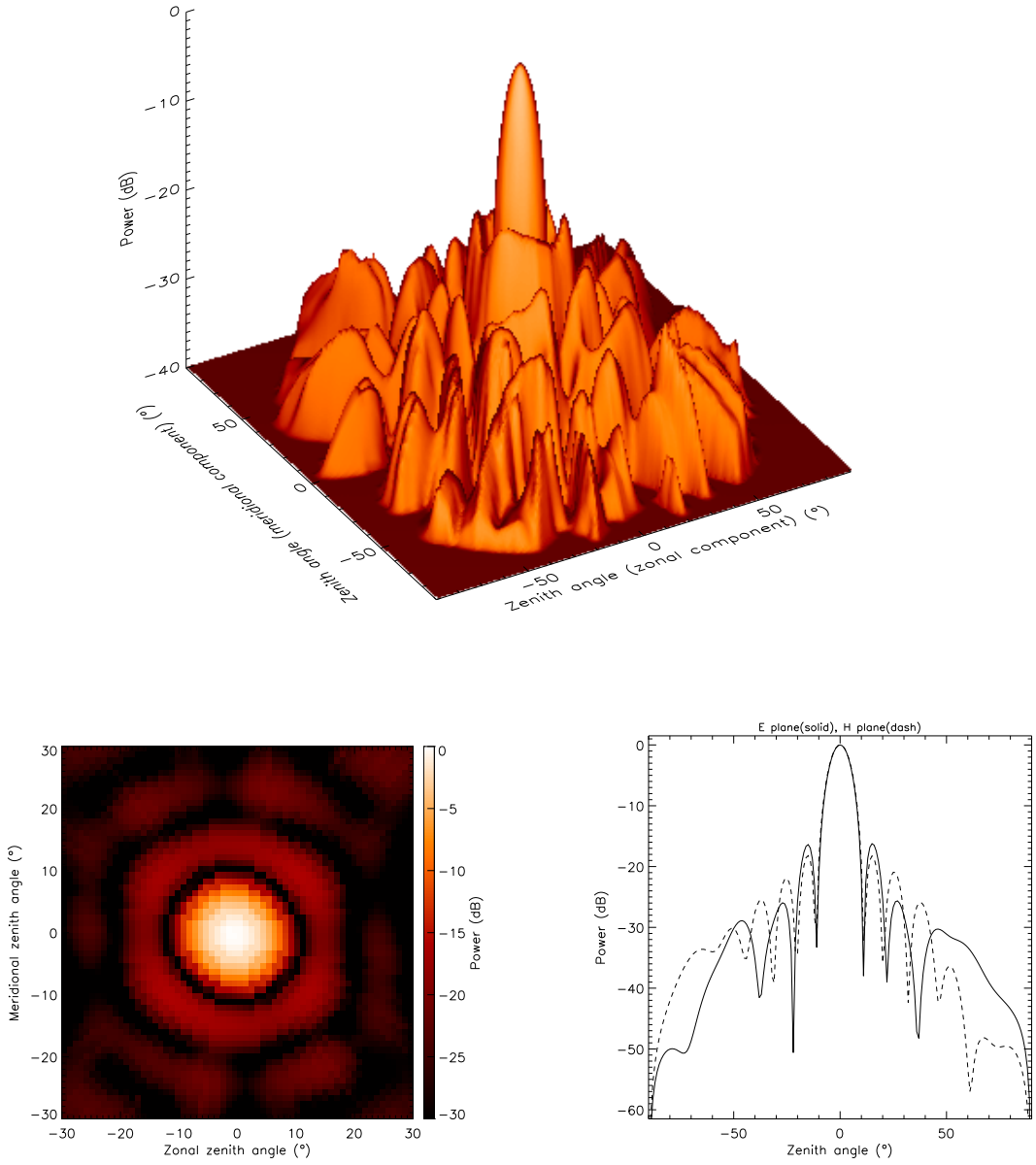

Figure 2.4: Modelled transmitted beam pattern of the MF radar using seventy-eight north-south aligned dipoles. The upper diagram is a three dimensional representation of the beam pattern. The lower left diagram is an image contour over a restricted zonal and meridional zenith angle. The lower right diagram is a cross section of this pattern with the E-Plane (solid) and H-Plane (dashed) indicated.

2.2.2 Description of the MF Doppler radar transmitter and receiver system

The current MF Doppler radar system hardware comprises three transmitter chassis and one receiver and data acquisition (RDAS) chassis [*Reid et al.*, 1995]. Each of the transmitter chassis are self-contained and can operate independently if desired when mated to an appropriate receiving system. Both transmission and receiving systems adhere to a modularised design philosophy and are formed from a number of fundamental channel units. Each transmitter chassis contains ten of these channel units (30 channels in total) and the receiving system contains 16 channels (with facility for additional channels). At a lower level, each transmitter channel comprises three primary modules; a Filter & Transmit-Receive (Filter/TR) switch module, Power Amplification (PA) module and a Phase Control (PC) module. This collection of primary channel modules is supported in each chassis by power supply, fan cooling and control interface modules. Similarly, each receiver channel is divided into a receiver module and signal processor module and these channel modules are supported by frequency synthesizer, range marker, power and control modules. The advantages of a modularised system layout are numerous and include reduced construction costs, standardised channel operation and ease of maintenance. An IBM-compatible personal computer (PC) running MS-DOS controls the function of the transmitter and receiver system and a second computer running Linux stores and analyses the data collected. Figure 2.5 is a composite photograph of the transmitting, receiving and computer systems that compose the MF Doppler radar.

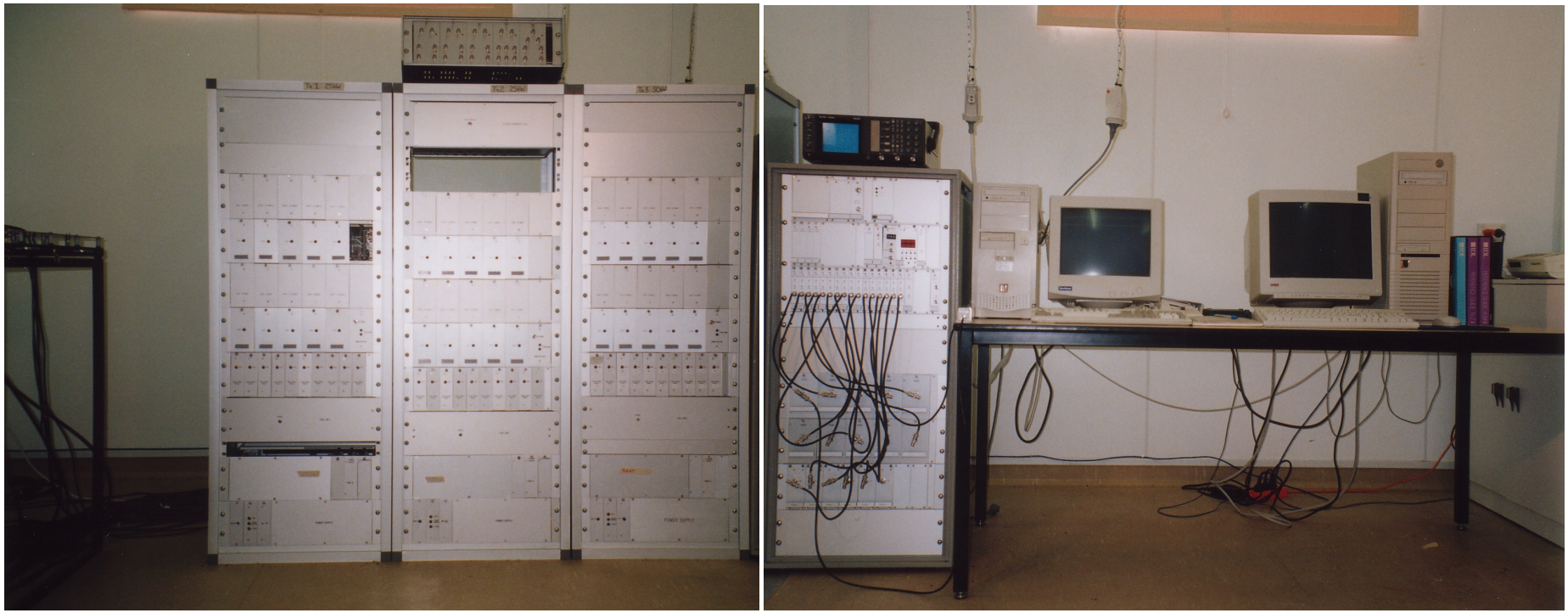

Figure 2.5: The 1.98 MHz Doppler radar system. A composite photo of the transmitting, receiving and computer components that form the complete radar system. The system comprises (from left) antenna patchboard (partially shown) three transmitter chassis, one radar data acquisition system (RDAS), the radar controller computer (Medusa) and a data analysis computer (MF). The portable power combining system described in Chapter 4 is shown on top of the middle transmitter chassis and directly underneath this is a fixed 10:1 non-asymmetric power combining system. Shown above the RDAS chassis is a cathode-ray oscilloscope used for general monitoring duties.

The transmitter chassis are nominally identical except for the 5.0 kW power amplifier modules of the third transmitter (third chassis from left in figure) and the 10:1 power combining system installed in transmitter chassis two (second from left in figure) for non-asymmetric operation into a 50 Ω load. The capability of this system as pictured in Figure 2.5, is detailed in Table 2.2.

Parameter	**Specification**
	Transmitter
Carrier frequency	1.98 MHz
RMS PEP power	92 kW
Average power	184 W[a]
Power aperture product	2.9×10^8 W m^{-2}
Pulse shape	Gaussian
Pulse width (3 dB)	$\sim$20 μs
PRF	1-100 Hz
Duty cycle	$<$0.5%
Transmitted beam width	$\sim10^\circ$
Beam directions	Full hemisphere[b]
Polarisation	Linear[c]
Pulse coding	Phase modulation (0, π)
Transmitter channels available	1-30
	Receiver
Frequency	1.98 MHz
Selectivity/Bandwidth (3 dB)	$\sim$80 kHz
Receiver channels available	1-16
Sensitivity	$\sim$0.3 μV
Gain	40-100 dB
Signal processors	Coherent (In-phase, Quadrature)
Resolution	12-bit
Sampling height interval	2 km

[a] Assumes a PRF of 100 Hz.
[b] Increased beam width at zenith angles $\gtrsim30^\circ$.
[c] O or X can be manually configured at the present time.

Table 2.2: MF Doppler radar system characteristics.

A common method of comparing the overall radar system capability is by using the power aperture product $P_{AP} = P_{pk}A$, where P_{pk} is the transmitted peak power and A is the effective antenna area. This term is a useful measure because the power

received via a reflection from a large surface or refractive index discontinuity, which is stratified perpendicular to the radar wave propagation is proportional to the product of these two terms [*Röttger*, 1989*a*]. And the optimization of the received power is of paramount importance in radar design. Typical values for MST radars fall within the range $10^6 - 10^{10}$ W·m^2 [*Gage & Balsley*, 1978]. The configuration of the system was varied for the actual meteor experiments (described later) and the details of this specific configuration is indicated in Table 6.3 of Chapter 6.

The fundamental operation of the MF Doppler radar is described in more detail using Figure 2.6.

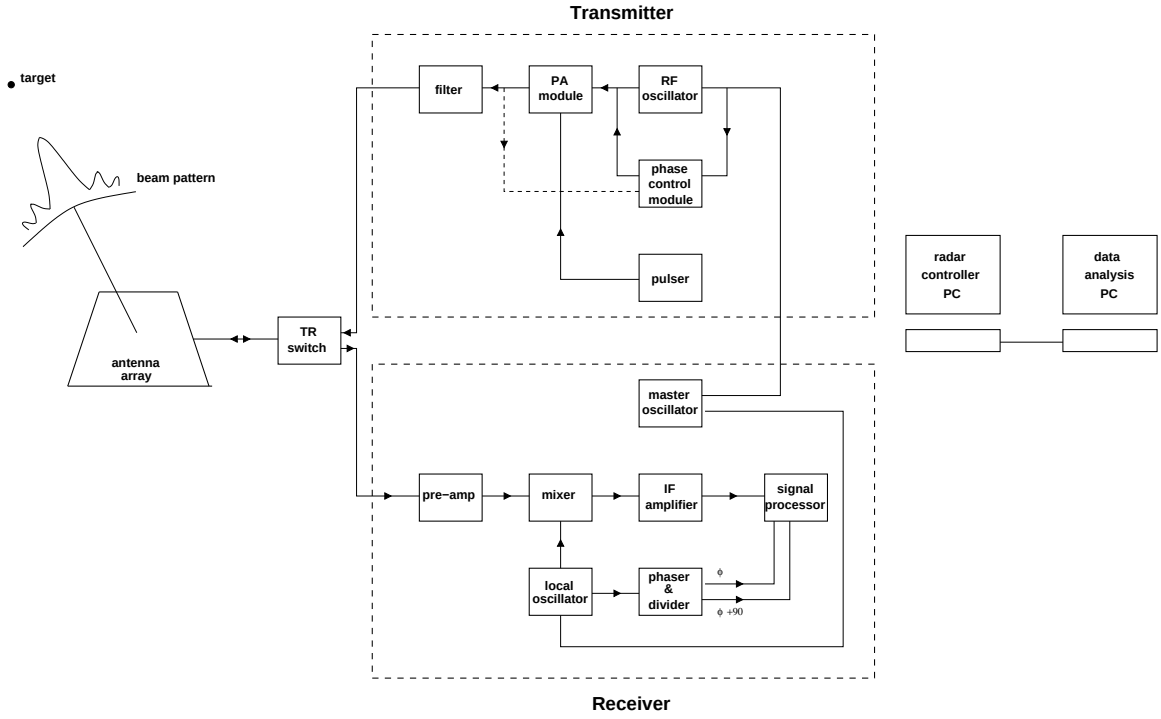

Figure 2.6: MF Doppler radar block diagram.

The physical size of each transmitter chassis is 1435 mm (h) × 550 (w) × 450 (d), and the operation of each channel within the transmitter chassis is identical. A channel's operation centres around the function of the three primary transmitter modules and the transmitter frequency is controlled from a frequency synthesizer (or master oscillator) located in the RDAS receiving system. The PA module produces either a nominal 2500 Watt (2.5 kW module) or 5000 Watt (5.0 kW module) square wave into

50 Ω via a class-D mode of operation, which theoretically can approach 100% efficiency with typical duty cycles and currents [*Hagen*, 1996]. This PA output is pulse modulated to produced a Gaussian-shaped envelope whose width can be manually adjusted to give a fixed pulse width over the range of 13 to 30 μs. This PA module's output is then filtered within the Filter/TR switch module to remove the higher order odd harmonics of the square wave and retain the 1.98 MHz fundamental sine wave.

The beam steering capability of the radar is achieved by individually phasing the output of each transmitter channel. This operation is managed by the Phase Control module contained within each channel, each of which in turn is linked to the master oscillator for phase referencing. The Phase Control module takes a voltage sample from an inductor within the Filter/TR switch module to establish the phase of the final signal delivered at the channel outputs. The phase of this output signal is compared with the signal input to the PA amplifier and the RF drive signal is adjusted to bring the channel output signal to the desired phase. There are two cases where a phase adjustment is necessary. Firstly, the output of each channel is calibrated during the phase zero cycle to achieve the same relative output phase over all channels. This is completed before an acquisition cycle and initialises the phase of each channel in readiness for vertical beam transmission or for the second process if required. The second process steps the phase of a channel relative to the others in order to obtain the requested beam direction.

Atmospheric sensing radars commonly use Gaussian shaped pulses (in preference to square, trianglar, smoothed trapezoid etc.) to optimise signal return while minimising sidebands and interference in the increasingly congested radio spectrum. An example of a typical Gaussian modulated pulse channel output from a 25 kW chassis is displayed in Figure 2.7. This is the output signal as measured at the Filter/TR switch antenna output through a 25 Ω attenuating load. Channel output of the 50 kW chassis exhibits a similar Gaussian shape albeit with an increase in peak-to-peak voltage.

As mentioned above the RDAS contains receivers and signal processors for 16 channels. As is the case in the transmitter chassis, the modular construction allows

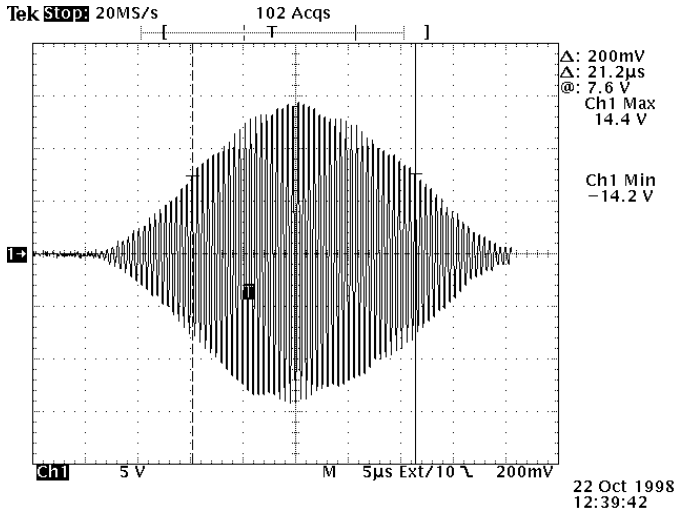

Figure 2.7: Transmitted pulse waveform. An example of typical output from a 2.5 kW channel of a 25 kW transmitter chassis. The apparent complex structure displayed is an artifact of the digital storage oscilloscope and no distortions are actually present in the waveform's fine structure.

the upgrading and easy interchange of primary receiver components as necessary. Here, there are two distinct receiver types (type 1, channels 1-10 and type 2, 11-16) feeding standard signal processor modules. The physical size of the RDAS chassis is 1180 mm (h) $\times$ 550 (w) $\times$ 500 (d).

The receiver module's purpose is to provide sufficient amplification of the weak reflected signal from the radar target as excited on the arrays dipoles and reject all other RF signals. These functions are encapsulated in the three primary receiver parameters of amplification (gain), selectivity and sensitivity and are tabulated in Table 2.2. To accomplish this task, most radar receiving systems utilise a particular implementation of the superheterodyne type receiver design, and the two receiver types of the MF system are no exception.

The principal operation of the superheteordyne receiver is to convert the information contained within the modulated RF carrier to a fixed frequency where it can be better amplified and processed (e.g. *Tsuda* [1989]). Essentially, after the transmitted signal is isolated from the receive section via the Filter/TR switch, any received RF signal is pre-amplified in a radio frequency amplifier located at the input section of the receiver. This signal is then mixed with a coherent Local Oscillator (LO) signal and

lowered in frequency to an Intermediate Frequency (IF) signal. This IF signal is then amplified as required and then detected within the signal processor as in-phase and quadrature signals via re-use of the local oscillator signal. These two analogue signals are digitized through an Analog-to-Digital converter (ADC) for eventual transfer to the radar controlling computer as a complex time series.

Expanding on this receiver system outline in terms of the MF Doppler radar used for data collection, the input impedance of the receivers (50 Ω) is ideally matched to the 2 MHz output of the Filter/TR switch to facilitate maximum power transfer from dipole(s) to receiver. At the input stage of the receiver the low-noise RF amplifier (or *preselector*) increases the weak RF signal to a manageable level and provides some filtering via a pass band to increase its frequency selectivity amongst the congested RF environment in which the signals propagate. This amplifier section also isolates the LO from being coupled to the antenna, where it could be radiated and cause interference with the target signal [*Carr*, 2001].

In the following mixer stage the amplified RF signal is combined in a nonlinear circuit with the local oscillator signal (2.435 MHz). This local oscillator frequency is most often made higher than the RF signal (termed *high-side injection*) although theoretically it is an arbitrary choice. A group of frequencies will appear at the output of the mixer of the form f_{LO}, f_S and $nf_{LO} \pm mf_S$ where n and m equal $0, 1, 2, \ldots$ [*Carr*, 2001]. In most circuits n and m are zero and unity so that four primary frequencies are obtained, the fundamentals, f_{LO}, f_S, and the second-order products, $f_{LO}+f_S$ and $f_{LO}-f_S$[2]. Most receivers retain the difference frequency for the intermediate frequency, in this case 455 kHz, with all unwanted mixer products filtered by a pass band centred on the chosen IF. The signal at this intermediate frequency contains the same modulation as the original carrier and hence the information about the target can be extracted [*Kennedy*, 1970]. The bandwidth of the radar receiving system is established by the fixed-tuned bandpass filters in the initial stages of the IF amplification section. As

[2]If the two inputs contain harmonics then there will be additional frequencies in the output of the (nonlinear) mixer.

the IF amplifier is optimized for a single, lower frequency, it is able to produce very high gain without oscillation and other unwanted by-products. Also, because the amplification is more easily applied at this lower frequency a more uniform performance can be achieved across individual receiver modules.

The same frequency syntheziser that provides a constant oscillator to derive the transmitted carrier wave provides the same phase information for injection at the receiver and signal processor. The local oscillator is first used in the superheterodyne receiver and subsequently in the signal processor. It is this arrangement that makes the detection process coherent. and ultimately provides the amplitude and phase of the received signal.

The operation of the signal processors and final reduction to target amplitude and phase can be described as follows. If we classify the narrowband signal output from the IF amplifier as $s(t)$ where

$$s(t) = A(t)cos[\omega_O t + \phi(t)] \tag{2.1}$$

then ω_O represents the IF carrier frequency, A(t) and $\phi(t)$ represent the narrowband (relative to ω_O) amplitude and phase modulations, respectively [*Lewis et al.*, 1986]. In this formulation any phase modulation of the transmitted signal, Doppler effects and constant phase shift is contained in the $\phi(t)$ term. Within the signal processor module the signal s(t) is divided into two; one component is mixed with the local oscillator signal $cos\omega_O t$, while the other with the LO signal shifted 90°. The result of each is then lowpass filtered. The two components obtained by this mixing process are termed the *in-phase* ($I = \frac{a}{2}cos\phi$) and *quadrature* ($Q = \frac{a}{2}sin\phi$) components. The constitutes the signal information being removed from the IF carrier and thus constitutes a coherent detector. These separate signals are then digitized in the 12-bit ADC. Because the two components are orthogonal, a sample of each at any time t can represented by the complex number $I + jQ$ where j is $\sqrt{-1}$. Consecutive complex samples form a time series for each range gate required and this is the form in which the data is stored from an acquisition. The amplitude and phase of the signal can then be recovered using the

relations

$$A = (I^2 + Q^2)^{1/2} \tag{2.2}$$

$$\phi = arctan(\frac{Q}{I}) \tag{2.3}$$

For a pulse repetition rate of 100 Hz and an acquisition period of 2 minutes over multiple heights and receivers there is the potential to accumulate data sets of the order of 10 MB. To alleviate the load on the radar controller and analysis computer for a particular atmospheric application, this data set size can be reduced via coherent integration [*Röttger*, 1989*a*]. Here a suitable number of contiguous samples (separate in-phase and quadrature) are averaged. *Röttger* points out that the integration period must be shorter than the typical time scale of signal variations due to the fluctuating scatter process as well as due to the frequency changes resulting from the bulk motions of the scattering of reflecting medium. An alternate reason for applying coherent integration is for an improvement in signal-to-noise ratio (SNR). This offers an an improvement in the SNR by N, where N is the number of samples averaged [*Tsuda*, 1989], [*Hocking*, 1989].

In terms of the applying coherent integration in this study two determining factors were highlighted. As computer network speed increases, the ability of a radar to cope with larger streams of data is increased. This affords the opportunity to record data without coherent integration and select the level of coherent integration required post acquisition. Thus different reduction analyses can be completed on the core data as it may be more applicable to have minimal coherent integration in one analysis case and heavy coherent integration in another. The facility to apply different reduction analyses to a single data acquisition increases a radar's flexibility and widens the opportunity for later analysis. In addition to this consideration is the later described desire to deduce speeds from the meteor events detected. Over the low pulse repetition frequencies used at MF, the target's phase behaviour changes rapidly and thus coherent integration will remove valuable information. It was for these two reasons that coherent integration was not applied to the radar data collected in this case.

In terms of computer control of the radar hardware, all three transmitter chassis are linked to the RDAS via a 50-way ribbon cable and a serial RS232 line. An interface between the RDAS and the radar controller computer is achieved by a 32-bit, parallel, digital I/O card. The radar controller (*Medusa*) manages the radars functions via this interface through an executable running under MS-DOS. The radar controller PC is then networked to the radar analysis PC (*MF*) whose primary function is to perform selected analysis on the acquired data and/or bulk data storage. This radar analysis PC is in turn part of a Local Area Network (LAN) encompassing all atmospheric sensors at the BP field site. Communication to the field site from the University of Adelaide is provided via a microwave communication system, and configuration of radar acquisition parameters can be achieved remotely through the *radarcfg* software. This programme can be run on any networked Linux PC and enables all typical experiment parameters to be manipulated for a specific antenna and Tx/Rx hardware configuration. Raw or analysed data files can be archived to CD-R.

2.3 Improvements and hardware additions to the MF Doppler radar system

The MF radar system had operated almost continually for a number of years at the Buckland Park research facility site. The system modifications and additions described in the following section were instituted after a lightning strike to the MF antenna array temporarily halted atmospheric observations. This enforced break in data collection afforded an opportunity to thoroughly investigate whether the recent performance of the MF radar system was within specification. It was during such investigations that progress was made on some established system shortcomings and a number of hitherto unknown problems were uncovered. Specific areas addressed in this radar maintenance programme were suspected power and phasing problems of the transmitter; the integration of the third, 50 kW, transmitter into the radar system; the leakage of the transmitted pulse into the receivers along with other minor transmitter system faults.

Some concerns with the receiving system were attended to also, as were data transfer problems between the radar controller PC and analysis PC that emerged. New hardware was also integrated into the radar system in order to enhance its capabilities in the form of a purpose built power combining system. Future directions in relation to the current radar hardware, maintenance and calibration procedures are also discussed. Each area is discussed in terms of isolating the underlying problem or fault then tailoring and implementing an appropriate solution.

During a nearby thunderstorm on the 12th of January 1998 a section the MF antenna array was struck by lightning. Later investigations indicated that the balun affixed to support pole 10EN5[3] showed extensive damage consistent with a lightning strike, with the balun Printed Circuit Board (PCB) being totally destroyed and the southern section of the north-south (NS) oriented dipole being grounded. Some receivers were found to be non operational. It was apparent that further internal damage had occurred to the RDAS and this system component was returned to the manufacturer for fault diagnosis and rectification. Their investigations confirmed numerous faults within this system. A new interface card was installed and faults in the data sequencer, frequency synthesizer amongst other faults, were rectified. Minor damage to the transmitter power supplies, which may have been a direct result of the strike or indirectly from the loss of mains power to the entire BP research facility at this time, was also repaired. The subsequent repair of the RDAS allowed a more detailed inspection to commence on the transmitting system.

2.3.1 Power and phasing problems & solutions

Data gathered by a malfunctioning radar system and the subsequent analyses applied post acquisition may be expected to exhibit symptoms of any developing hardware faults. However, the data gathered from this system in its routine mode of operation (e.g. Full Correlation Analysis (FCA) wind and Differential Absorption Electron (DAE) concentration estimates) had passed the necessary quality control criteria up

[3] 10^{th} array row, **E**ast**N**orth, 5^{th} array column.

until the lightning strike. One advantage of the FCA analysis is that it requires only a vertically directed beam and it is relatively insensitive to variations in that transmitted beam width (e.g. *Røyrvik* [1989]). Similarly, because phase critical parameters are not utilised directly in FCA analysis, save as a by-product, if adversely affected they do not contaminate essential data reduction. Because of this, the accumulated routine analysis output parameters are not always sensitive to certain vagaries of system behaviour to act as accurate radar performance indicators. Even a reduction in transmitted power (by the automated precautionary shutdown of power amplifier modules) is tolerated and only has a significant effect on analysis outcomes when a critical number of channels are removed from contributing to total output power. In contrast to this situation, when the radar is configured for more demanding research (in terms of hardware and subsequent analysis complexity), possible suggestions of abnormal behaviour become more apparent.

When the system was configured for scatter aspect sensitivity investigations via limited beam steering around zenith, it was found that some off-zenith beam directions did not exhibit the expected echo power reductions [*Holdsworth*, 2002, private communication]. This result is contrary to the angular spectrum increasing with height [*Reid*, 1990].

This may be interpreted as an indication of a broader beam being transmitted than that expected. But other explanations carry equal weight, such as contamination by other dynamic phenomena of the upper atmosphere, echoes from sidelobes, or the aliasing of structure at a greater range, etc. These points serve to illustrate the difficulty in examining routine analysis and specific experiment results in terms of confirming normal radar operational behaviour.

More specifically, because of the dynamic nature of the middle and upper atmosphere, confirming radar hardware performance to specification is fraught with difficulties when this atmospheric system is included in any measurements. A focus on the radar hardware operation alone (*sans* atmosphere) offers a more tightly constrained system in which to evaluate performance.

Examples of abnormal hardware behaviour had been accruing for sometime. Typical instances of this were often apparently confined to the Phase Control (PC) module. These modules would cease to function in their task of initialising each channels relative phase and in the programmed incrementing of their phase, only to perform at a later time or when re-positioned into in another transmitter channel. A number of possible causes of this module's range of behaviour have been put forward. Firstly, strong wind gusts directed over the array at surface heights cause the dipole antenna impedances to vary significantly[4] which may in turn affect the Filter/TR switch current sample used in the PC module's initialisation process. The quasi-random nature of this possible cause may explain the supposed erratic behaviour observed, but if true, would be a concern for normal radar operation. Secondly, it was thought that the radar control room's ambient temperature combined with the heat generated within the transmitter chassis may affect some critical RF components in a manner that affects normal radar operation. The ambient temperature influence on receiver operation (in a non-airconditioned control room, exposed to daily temperature fluctuations) has been documented [*Vandepeer*, 1993] for a previous system configuration and while receiver operation may be more susceptible to temperature variations, it is reasonable to assume that some thermal influence is exerted upon the transmitter chassis as well. However the current radar hardware is housed in an air-conditioned room that appears to adequately remove excess heat. Alone or collectively, neither of these explanations adequately address all abnormal behaviour observed.

This absence of consistent PC module behaviour served also to compound the effectiveness of the manual calibration that was periodically applied to each channel. This calibration often degenerated into a trial and error process that often ultimately was unsuccessful in calibrating all PC modules for an extended period. Additionally, there was a sporadic occurrence of PC module faults that appeared to have an influence over an adjacent channel's operation. This apparent channel crosstalk was intermittent and thus its source could not be isolated.

[4]Also observed at other radar sites (e.g. *Brown* [1992]).

The cause(s) of these symptoms may be distributed throughout the complete radar system. In an effort to isolate specific causes of the observed ailments, the complete MF radar system was sectioned into its constituent components of, transmitter, antenna array and receiver. Each system was then examined individually for behaviour outside of specification, with underlying causes traced and faults repaired. This approach was deemed to be an efficient use of the resources available as it reduced a relatively complex system and possibly widely distributed fault sources to smaller, more manageable systems, that could be addressed flexibly, as resources permitted. For instance, sources of the phasing problems mentioned above may not only be confined to the transmitter section of the radar but may emanate from within the the coaxial cable system feeding each antenna. These cable sections have experienced water ingress in the past which is an example of one mechanism which could modify the phase behaviour of radiation on transmission and that recorded on reception. Similarly, faults developed in the balun circuit or its associated connections can affect radar performance. This illustrates that any phasing problem may have an antenna array component and due to the size of the antenna array (178 dipoles), supports an approach that addresses the primary systems separately. The results of the investigations into the antenna array component are thoroughly discussed in Chapter 3, while the investigations into the transmitter and receiver system are discussed in the following sections.

To facilitate the extensive maintenance undertaken on the various modules of each channel within the MF radar, a set of thirty dummy loads was required to be designed and constructed [*Woithe*, 1998, private communication]. It was also envisaged that these loads could later serve during radar calibration procedures throughout the operational life of the radar. Each load would be representative of a typical antenna group impedance (nominally 25 Ω $\angle 0^{\circ}$) and connect directly to the Filter/TR switch module Input/Output (IO). In this configuration the load would be required to dissipate the power output of each radar channel (nominally 2.5 kW for transmitter chassis one

(Tx-1), Tx-2 and 5.0 kW for Tx-3) without component breakdown throughout continual operation. Additionally, the load was to provide an approximate 20:1 attenuation of the channel power output to enable possible signal examination via a Cathode Ray Oscilloscope (CRO) or Digital Storage Oscilloscope (DSO) without overloading the input section of these devices. Individual loads contained a network of 100 Ω, $\frac{1}{4}$ Watt resistors on a PCB with a male Bayonet Nut Connector (BNC) for connection to the Filter/TR switch module. Ten of the loads had a length of coaxial cable attached for easy patching to a monitoring CRO/DSO for channel output observations. The loads exhibited |Z|=25.0±0.5 Ω, ∠Z 1.8°±0.4°. Individual dummy loads were numbered according to their respective transmitter channel and remained with this channel, where possible, throughout testing. A load was also manufactured for connection to the output of the PA module. A similar design to that used in the Filter/TR switch load was employed for this application, aside from exhibiting the nominal 50 Ω ∠0° impedance requirement for connection to the PA module output. An output attenuation of 20:1 was also achieved with this load.

In an effort to provide definitive evidence of the claims outlined previously and to gain an overall perspective of the scope of the transmitter system's deficiencies, output from each channel of the three transmitters was measured. Table 2.3 displays the result of these measurements. The format of this table perhaps best summarises the state of the MF transmission system at any moment in time and will be used at various junctures to summarise the effectiveness of the maintenance techniques applied to the system.

Transmitter	**Channel**	**Amplitude** [Volts]	**Amplitude Reference** [Volts]	**Phase** [ns]	**Relative Phase Behaviour** ch lag/lead ref ch
1	1	13.0	-	-	-
	2	13.0	13.0	4	2 lags REF
	3	13.0	13.0	2	3 leads REF
	4	4.5	13.0	negligible	
	5	13.0	13.0	◇	◇
	6	11.5	13.0	20	6 lags REF
	7	11.5	13.0	90	7 lags REF
	8	<13.0	13.0	24	◇
	9	14.0	13.0	20	◇
	10	<13.0	13.0	10	◇
2	1	30.0	-	-	-
	2	20.0	30.0	16	◇
	3				
	4				
	5	30.4	30.0	10	◇
	6	28.8	29.8	14	◇
	7				
	8				
	9	29.8	30.0	10	◇
	10	30.0	30.2	10	◇
3	1	3.12	-	-	-
	2	2.08	3.12	7	2 leads REF
	3	2.36	3.88	25	3 leads REF
	4	1.04	2.96	27	4 lags REF
	5	1.72	3.56	<10	5 leads REF
	6	2.60	3.50	10	6 leads REF
	7				
	8	0.64	3.16	10	8 leads REF
	9				
	10				

Table 2.3: Pre-maintenance transmitter channel amplitude and phase values using a vertically directed transmit beam. Measurements were recorded at the Filter/TR switch module outputs through a matched dummy load and represent (in general terms) the state of each channel of the transmission system prior to the maintenance procedures described in the text. *Amplitude* is the peak-to-peak measurement of the transmitted waveform of the respective channel as monitored through the attenuation of the dummy loads except Tx-1 values which is nominal amplitude. The *Amplitude Reference* is a measurement of the reference (REF) waveform's behaviour (i.e. channel 1 of each transmitter) over consecutive channel measurements. *Phase* is the relative phase difference of the output waveforms. If the Phase is termed *negligible* then a phase measurement was unobtainable due to DSO bandwidth limitations. A symbol (◇) denotes a parameter available but not recorded at the time due to the initial non-standardisation of system performance classification. A blank entry denotes a severely malfunctioning transmitter channel and thus no measurement could be made. Examined collectively, this table shows the inconsistent power and phase behaviour of the transmission system as a whole. This table should be compared to those obtained at the conclusion of the maintenance period. The measurement processes used are documented in *Woithe & Grant* [1999].

To fully explain the content of the table it is necessary to briefly touch upon the operation of the radar's external triggering module. As a result of the maintenance conducted on the system it became apparent that each transmitter chassis was not identical (excluding the higher power 5.0 kW PA modules of the third chassis) and that each chassis exhibited circuit idiosyncrasies in specific areas (e.g. within PC modules, Filter/TR switch modules etc.). One area in which the transmitters differed in their operation was their external CRO trigger circuit. This circuit provided a trigger from a port on the front of each transmitter chassis that allowed connection to the external trigger input of a monitoring CRO/DSO. This greatly facilitated the general maintenance and recording of the transmitters behaviour but resulted in minor variations in the values tabulated. Specifically, the point at which this external trigger pulse ended marked the centre of the transmitted waveform (measured at the Filter/TR switch module output). This was the nominal behaviour of the circuit and it was found that there were significant differences in this circuit across the three transmitters. The result of this was that often the amplitude measurement was not located precisely at the centre of the waveform. As these differences were uncovered while maintenance progressed, the preliminary amplitude measurements are more prone to transmitter external trigger module dependencies than later values. This initial variation is apparent in the amplitude measurements of Table 2.3 and indicate that amplitude comparisons in this particular table are best undertaken within the individual channels of the respective transmitter chassis rather than over separate transmitter chassis. One maintenance aim was to standardise each *nominally* indistinguishable radar component. A reason for addressing this variation was to allow a better performance comparison between channels and transmitters. This approach improved the consistency of later tabulated amplitude measurements, but did not completely eradicate the external CRO trigger problem within the maintenance period. It should be noted that the internal transmitted pulse triggering mechanism, responsible for RF pulse generation, was consistent over all the transmitter chassis' and thus offered no significant source of discrepancy.

A reference channel in each transmitter was chosen primarily in order to compare relative channel phases but also to observe amplitude output over time. Channel one of each transmitter was examined and confirmed to be performing as close to specification at each stage of maintenance before being used as the transmitter reference (REF).

In terms of the amplitude output of the radar, it can be seen that a number of channels across all transmitters were down on power relative to the assumed nominally performing channels. For instance within Tx-1, channels 6 and 7 are under-performing and channel 4 has a significant fault that is mainifest as a 9 dB voltage reduction. Of the working channels from Tx-2, channel 2 has a 3.5 dB voltage reduction and in relation to Tx-3, if channel 1 is assumed to be functioning nominally, then all other channels are below expected power output levels.

In analysing the amplitude reference behaviour, the results of transmitter one (Tx-1) offer no fine scale fluctuations. These particular data entries were approximations taken during the very early stages of the maintenance program before measurement practices had been standardised and as such only represent the nominally consistent behaviour of channel one, Tx-1. However, the available data for transmitter two and three shows variation of the reference channels output over the measurement of adjacent channels. This behaviour is thought to be a result of both minor variations of the external trigger signal and small variations in the PA module power output. These particular fluctuations in PA module output are in themselves not thought to be indicative of any PA module faults and if viewed as typical PA module behaviour perhaps represent normal operational fluctuations due to inefficient heat extraction and slight variations in mains power. This variation could be used to more accurately model the output power of the radar over consecutive acquisitions and as such could be included in future beam modelling.

The relative phase between a selected and reference channel waveform was also recorded (the procedure is detailed in *Woithe & Grant* [1999]). It was assumed that the small amplitude variations in channel output over time mentioned previously had a negligible affect on the recorded phase difference of the channels. Each transmitter

channel is specified to have a phase control resolution of 8.5° steps (i.e. 12 ns @ 1.98 MHz) and a phase control accuracy of within 4° of the desired delay. At the transmit frequency of 1.98 MHz this translates to each channel having a waveform output within ±6 ns of the nominated phase due to each channels calculated phase step required to achieve a vertical transmit beam bore sight. For such a beam, all transmitter channels have the same relative phase offset of 0°, thus each channel should lag or lead the reference by $\leq$ 6 ns.

The phase values listed in Table 2.3 indicate that most channels of all three transmitters have an output that does not conform to system specification. Only channels two and three of transmitter one are strictly within phase specification. On the other hand, six channels display a phase value $\geq$ 20° with channel seven of transmitter one exhibiting a substantial 90° delay. Blank entries for a particular channel indicates that the PC module was not operational at the time the table data was sampled. This makes it impossible to measure the channel output waveform in this condition as the drive to the PA module is removed. This can have the effect of masking faults in the PA module or Filter/TR switch of a channel which can only be resolved with a fully functioning PC module. This was a primary reason for allotting all initial maintenance time to PC module fault investigation. Interestingly, it was found that more PC modules harboured faults than is indicated by the blank entries of this table, as some PC modules often remained functional in some respects while not actually performing completely as specified.

This investigation of the MF transmitting system indicates that it is performing well below specification in terms of both power and phasing criteria. Assuming that the onset of faults that contribute to these current performance parameters was gradual and not constrained to any isolated time period, the MF system may have been underperforming for some months. The power and phasing problems were investigated by tracking and addressing all faults in each of the main transmitter channel modules (PC, Filter/TR switch and PA module).

2.3.1.1 Phase control module

A vital component of a multi-channel, beam-steering radar is the phase shifting device that allows individual channel output to be varied. In the MF Doppler radar, this function was performed in the most part by the PC module. In a similar action to that initiated by the PA module in suspending channel output when an internal fault or external VSWR exceeds a known tolerance, the PC module curtails a channel's function if unable to self-calibrate its phase. For this reason maintenance attention was first directed to these particular transmitter modules in an effort to isolate faults locally first and thus later enable fault tracking through adjacent primary modules.

The design of the PC module had incorporated facilities on the PCB to allow for individual channel calibration. A successful calibration would allow the channel to 1) achieve the same relative phase as all adjacent channel (*phase zero*) and 2) increment the phase of an individual channel to obtain off-zenith bore sight beams (*phase step*). As mentioned previously, this calibration had often been a trial and error process as inconsistent calibration behaviour often masked core PC module faults. It was decided to ascertain the intended calibration technique inherent in the PC module design as a starting point for maintenance in order to classify individual PC modules as operational or faulty. This technique is described in detail elsewhere [*Woithe & Grant*, 1999] but is summarised here.

Dummy loads are fixed to the channel outputs to ensure a consistent nominal phase behaviour is maintained throughout the calibration process as the varying impedance of a connected antenna group often precluded successful calibration attempts. Previously existing calibration settings are erased (via a variable potentiometer) and new calibration settings monitored with a multimeter. Also monitored is the step waveform generated by the PC module board componentry. Provided this waveform adheres to certain criteria the variable potentiometer can be adjusted to a level that is higher that the waveform minimum but lower that the first discrete step. A successful phase zero will occur and phase stepping for an off-zenith beam direction may follow. Often

a step waveform that failed initial quality tests indicated a fault in the PC module.

As mentioned previously, one maintenance aim was to standardise *like* transmitter modules. Variations in nominally identical modules were to be eradicated in favour of the design specification or where this proved to be problematic, a revised and documented design. Reasons for this approach were two-fold. Any modern radar system (or electronic device in general) is modularised in an effort to optimise operation, cost and serviceability. In terms of the maintenance aspect, multiple identical modules that perform a specific function within the system are straightforward to repair and require a limited variety of replacement components because of their identical construction. Secondly, abnormal behaviour is more easily identified because normal operation is more strictly defined. This arrangement is particularly suited to RF systems that often have a less well defined performance envelope when contrasted to digital systems. This optimisation is radically diminished as individual modules within a group are modified. Because it was suspected that the PC modules harboured circuit variations (either design related or component related) an approach that adhered to maintaining this modular design edict was vigorously pursued. It was thought that only with such an approach could full operational status be restored to the system and actual intended circuit behaviour of the modules be critically evaluated. To this end all individual modules were numbered according to their transmitter and channel positions within the system. Each module remained in its position until all faults had been traced within that channel. It was only after modules of a particular channel had been declared fully operational that one of the primary advantages of a modular system could be utilised: the interchange of modules to aid further fault finding. This approach was in fact used extensively in the overall transmitter and receiver system maintenance programme. A byproduct of this maintenance approach and overall system design is that once all faults are eradicated, any new faults may be more easily tracked in the system. Previously this was not the case. Malfunctioning modules were swapped into new channels thus transferring erratic behaviour to often unaffected channels. Non-standardisation of the external CRO trigger circuit has been previously mentioned and another area

were this occurred on a much larger scale was within the group of thirty PC modules.

A total of eighteen types of faults within the phase control module or its motherboard (backplane) were uncovered. Some of these faults were isolated to specific PCBs, while others occurred on some or most modules. An itemised list of PC module faults is attached as Appendix A and displays all faults classified according to their likely origin. Each fault is documented in terms of fault, effect and action/remedy/solution. This list is detailed to assist in troubleshooting future faults sources and to enable the constructive evaluation of the circuit design. All references to component numbers are in accordance with the MF radar system technical documentation.

In the list detailed in the Appendix, mention is made of the faults occurring in the diode set D401→406. The role of this diode network is to clamp the current sample from the filter to between 0 and 5 V. It has been observed that if the current sample from the filter is fault free and the output from the eXclusive OR (XOR) gate immediately following the diode set is distorted or abnormal in some fashion, then the balance of the diodes is often asymmetrical. This is a common occurrence and a simple test has been devised to ascertain if these diodes need replacing and this is detailed in *Woithe & Grant* [1999].

It is speculated that this diode imbalance has been the hidden cause of a proliferation of modifications to the nominal 10 kΩ resistor (R406) connected to the calibration potentiometer. It appears that a correcting resistor (of various values) has been inserted in parallel to this 10 kΩ (R406) in an effort to achieve an acceptable calibration function. If the diodes are re-balanced and a 10 kΩ resistor is inserted in parallel to R406 then normal and consistent calibration will occur.

It appears that this diode section is moderately sensitive to the failure or reduced performance of one diode, possibly due to natural component attrition. Unfortunately, this can have a severe effect on a channel's ability to achieve phase calibration. However, the high number of other faults uncovered cannot be attributed to natural component attrition. Other module faults appear to have been present since manufacture and should have been addressed during an adequate testing phase following

system construction.

While the PC module is a core component of the transmitting system and the correction of all established faults within this module addressed many of the overall system concerns, it was apparent that further faults existed in those primary modules adjacent to the PC module that contributed to the observed power and phasing problems. Of these, the Filter/TR switch modules were to be examined next.

2.3.1.2 Filter/TR switch module

It became apparent through the interchange of functional and non-functional modules that part of the phasing problem was confined to the Filter/TR switch modules. The design and development of this particular Filter/TR switch module is detailed by *Vandepeer* [1993]. Due to the specific Filter/TR switch circuit design being available, it was thought useful to measure the actual characteristics of each of these modules and compare them with the expected theoretical values, as well as with the channel's phase behaviour, in an attempt to correlate observed Filter/TR switch parameters with poor channel performance. These measurements are displayed in Table 2.4. The technique to obtain these measurements has been detailed in radar maintenance documentation [*Woithe & Grant*, 1999] with a view to becoming a scheduled part of radar maintenance.

Channel characteristics were compared against the overall group values and with their expected theoretical values so as to isolate any significant deviations from established nominal characteristics. It can be seen that channels 2,7,8,9 and 10 have marked deviations in L1 and/or L2 values. This deviation may be interpreted as a source of, or a contributing factor in, the abnormal phase delay recorded for those channels. Specific modifications to the Filter/TR switch inductors of some of these channels were proposed in an effort to align a channel's actual behaviour to be closer to theoretical specification and thus correct their abnormal phase delay characteristics (see Table 2.5). The positive effect the modifications have had on the phase behaviour of the respective channels is highlighted in Table 2.6 and is manifest as a reduction in

Channel	**L1**		**L2**		**C3**		**Phase**
	$\|\mathbf{Z}\|$ [Ω]	$\angle\mathbf{Z}$ [°]	$\|\mathbf{Z}\|$ [Ω]	$\angle\mathbf{Z}$ [°]	$\|\mathbf{Z}\|$ [Ω]	$\angle\mathbf{Z}$ [°]	[ns]
theoretical	250	90.0	178.5	90.0	107.1	-90.0	0
CH1	245	88.9	184	88.1	99.7	-90.5	REF
CH2	246	88.9	170	88.3	99.4	-90.4	10
CH3	243	89.0	183	88.2	99.0	-90.4	fault
CH4	247	89.0	180	87.9	99.1	-90.4	10
CH5	246	88.9	176	88.3	99.8	-90.4	20
CH6	243	89.0	182	88.3	99.1	-90.4	fault
CH7	236	89.0	176	88.3	99.6	-90.3	fault
CH8	236	89.0	186	87.2	99.7	-90.4	17
CH9	239	88.8	179	88.5	99.3	-90.4	15
CH10	240	89.0	185	88.3	99.8	-89.9	7

Table 2.4: Filter/TR switch module characteristics before modifications. This table compares the theoretical complex impedance design values (L1, L2 and C3) of the Filter/TR switch module with the measured values from transmitter one before modifications were implemented. This information is correlated with the abnormal (out of specification) phase delay magnitudes measured for each respective channel. Channels 2,7,8,9 and 10 have noticeable L1 and/or L2 variations in comparison to other channels.

Channel	**L1**	**L2**
8	turn on	turn off
9	turn on	-
10	turn on	turn off

Table 2.5: Suggested modifications to selected channels of the Filter/TR switch modules of transmitter one in order to correct outstanding phase delay problems.

relative channel phase output. No improvement to channel two was possible due to the absence of an available tap for adjustment on the inductor L2. The abnormal phase behaviour of channels four and five is not attributed to faults that can be corrected by inductor modifications because of their closer adherence to expected theoretical values as detailed in Table 2.4.

Because of the inherent impedance stability of these hand-wound inductors, it is surmised that the tabulated characteristics are indicative of the long-term behaviour of the Filter/TR switches of transmitter one. This perhaps indicates that the theoretical impedance characteristics could have been more closely adhered to at manufacture.

To assist in the isolation of further problems in the Filter/TR switches a nominal signal was injected into the Filter/TR switch antenna input port and its output fed to receiver one of the RDAS. This receiver channel had been tested previously and found to be performing within specification. With the receiver gain set at 60 dB, the IF output of the receiver was recorded for a nominal input level of 10 μV. The result of this test is displayed in Table 2.7. From the table it can be seen that the receiver output of all channels of transmitter two are significantly below the nominal output of the reference channel (channel one, Tx-1). This result was found to be a symptom of Filter/TR switch modules with an over-stressed 150 μH choke located near the

Channel	**L1**		**L2**		**C3**		**Phase**
	$\|\mathbf{Z}\|$ [Ω]	$\angle\mathbf{Z}$ [°]	$\|\mathbf{Z}\|$ [Ω]	$\angle\mathbf{Z}$ [°]	$\|\mathbf{Z}\|$ [Ω]	$\angle\mathbf{Z}$ [°]	[ns]
theoretical	250	90.0	178.5	90.0	-	-	0
CH8	247	89.0	172	88.5	-	-	12
CH9	249	88.9	-	-	-	-	8
CH10	250	89.0	176	88.2	-	-	5

Table 2.6: Filter/TR switch module characteristics after modifications. This table compares the theoretical complex impedance design values (L1, L2 and C3) of the Filter/TR switch module with the measured values of selected channels from transmitter one after the modifications were implemented. Note the improvement of channel output phase behaviour.

Transmitter	**Channel**	**Filter/TR switch Input Level** [μV]	**Receiver IF Output Level** [V]
1	1	10	1.5
2	1	10	0.2
	2	10	0.2
	3	10	0.4
	4	10	0.8
	5	10	0.75
	6	10	1.2
	7	10	0.2
	8	10	0.7
	9	10	1.2
	10	10	1.2

Table 2.7: Filter/TR switch module I/O characteristics of transmitter two. This table displays the Filter/TR switch module output of each channel of transmitter two measured at the IF output of a receiver for a nominal input signal (10 μV). All channels display a significantly reduced output voltage. The first channel of transmitter one was used as a reference.

2 MHz Filter/TR switch output. It appears a significant voltage has over-stressed this component at some stage of radar operation. This problem was also present in the other transmitters. It was found that three channels of transmitter one and one channel of transmitter three had the same problem. All over-stressed chokes were replaced and normal transmitter performance restored. A simple test of the choke status in circuit was developed and is detailed in *Woithe & Grant* [1999]. This choke's apparent susceptibility to over-stressing and its deleterious effect on Filter/TR switch performance was of concern. A range of possible causes have been suggested. Because all chokes on transmitter two were faulty one suggestion was that the over-stressing was brought about by environmental factors such as high humidity. This particular transmitter saw service at the lower latitude site of Bribie Island for a number of years. However, this may not adequately explain the other transmitter's susceptibility to this ailment. Alternatively the failure of this component may correspond with the selection of a PRF $\geq$ 100 Hz. Anecdotal evidence indicates a possible correlation of choke failure with high PRF [*Holdsworth*, 1999*a*, private communication]. Interestingly

chokes were found to be missing completely from three Filter/TR switch modules. On at least two other separate occasions chokes failed. As the system was operating at or below 100 Hz in a mid latitude (lower humidity) air conditioned environment on these later occasions it is thought that the cause of the momentary high voltage experienced by the chokes is determined by factors other than high operating temperature. A mismatch of impedances in this section of the circuit is a possible cause of the higher voltage that leads to the failure of this component. Further operational testing is needed to isolate this particular fault. Additional performance tests where developed for the Filter/TR switch and one such test is detailed in the Appendix B.

Closer examination of the Filter/TR switches provided evidence of significant crosstalk between Filter/TR switch modules. It was determined that a low level atmospheric signal was present in the recorded time series (20 amplitude units peak-to-peak (Pk-to-Pk) compared to expected signal of 3000 amplitude units Pk-to-Pk) in some non-antenna connected Filter/TR switch modules due apparently to the operation of adjacent, antenna connected, Filter/TR switch modules (also observed by *Holdsworth* [1999*b*, private communication]). Assuming that these Filter/TR switches are adequately shielded from RF along their physical length in their chassis positions[5], a possible entry point for stray RF signal (possibly from adjacent coaxial cable feeders) is the normally unterminated output point to the receiver. While further investigation of this effect is warranted, the interim use of a low power tolerance matched (50 Ω) dummy loads on these unterminated connections during normal radar operation may reduce or circumvent the observed Filter/TR switch crosstalk.

Individual channel operation was not yet completely optimized however. Significant power abnormalities remained in numerous channels and attention was now directed toward the PA modules of each transmitter channel as the likely source of the outstanding faults.

[5]This has not been adequately investigated as yet.

2.3.1.3 Power amplifier module

Small reductions in amplitude output of a transmitter channel may be attributed to faults inside the Filter/TR switch but a dramatic reduction in expected output amplitude, when compared to adjacent channels (see Table 2.3), indicates the likelihood of faults existing within the Power Amplifier (PA) modules. The abnormal waveform output of the Filter/TR switch initially directed attention towards the existence of possible PA module faults but it was not until all faults within the Filter/TR switches had been eliminated and a suitable PA module load and test facility had been commissioned[6], that progress could be actioned in this specific area.

A typical symptom of divergent PA module behaviour is illustrated in the following two figures. Figure 2.8 displays two different transmitter channel outputs of a normally functioning system. The captured digital storage oscilloscope (DSO) trace shows the normal symmetric waveform output of a transmitter channel measured at the antenna port of a Filter/TR switch module and the slightly asymmetrical waveform output of a different transmitter channel measured at a 50 Ω load that terminated the PA module output. This waveform is typical of a properly functioning system in that its shape is yet to be finalised by a second stage of filtering that will occur in the Filter/TR switch module. This will result in a waveform output of similar character to the first waveform. The second figure (Figure 2.9) is in a similar format to the first except that it is apparent the PA module output is distinctly asymmetrical and limited in amplitude. A faulty power transistor was found to be the cause of this abnormal output waveform.

While documentation existed for the 2.5 kW Power Amplifier modules, minimal information was available for the uprated 5.0 kW modules. Essentially these up-rated modules had a doubling of power transistors on the same PCB as the 2.5 kW modules. Most significant power faults eminated from the PA modules of channels within the third transmitter chassis. Table 2.8 illustrates the extent of the problems detected in

[6]Comprising various modules from the 1.94 MHz SAPR (Spaced Antenna Partial Reflection) radar system. See *Phillips* [1989].

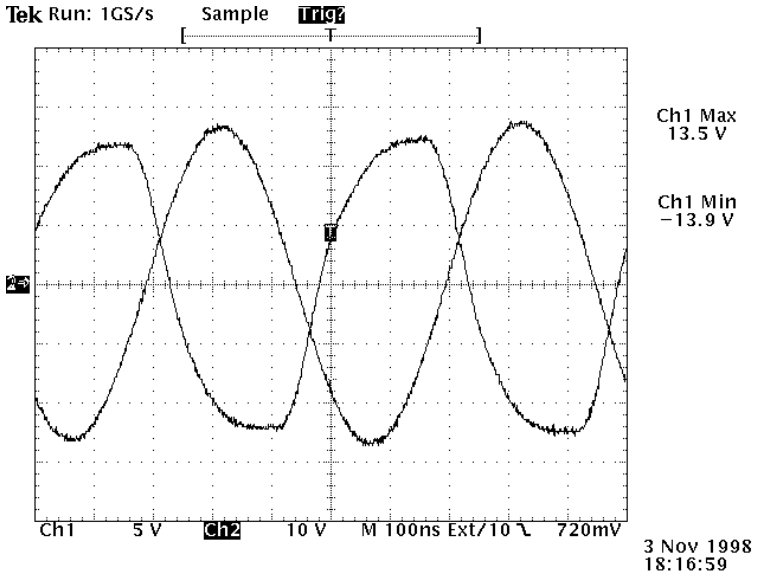

Figure 2.8: The expected output behaviour of a functioning 5.0 kW power amplifier module. The figure displays two different transmitter channel outputs. DSO channel 1 (5 V/div, 100 ns/div) displays transmitter channel 1 output as measured at the antenna port of the Filter/TR switch and highlights the normal symmetric waveform output. DSO channel 2 (10 V/div) (with the T mark indicating the DSO trigger point) displays the PA 10 module output into a 50 Ω load. The distinct asymmetry of this waveform is due to the filter process having not yet been completed. The initial square wave has had some harmonics removed but is yet to be filtered into the transmitted fundamental by passage through the Filter/TR switch.

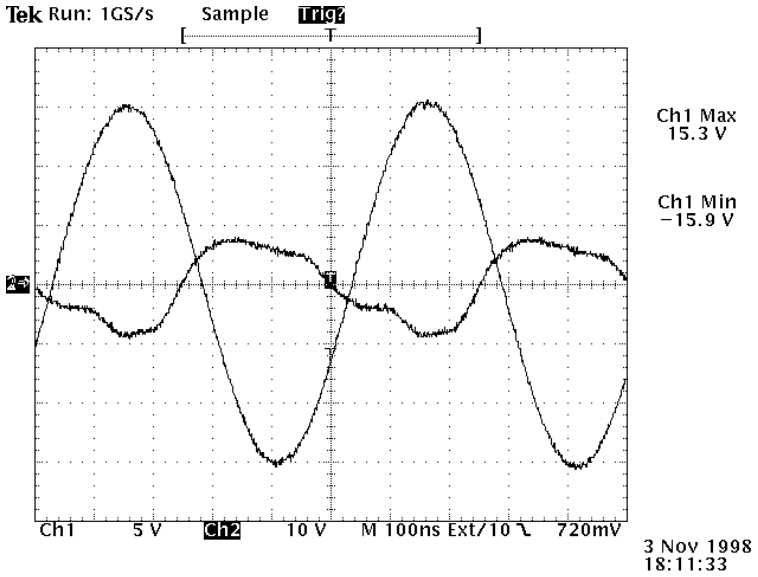

Figure 2.9: The output behaviour of a non-functioning 5.0 kW power amplifier module. A similar format to the previous figure is displayed. DSO channel 1 (5 V/div, 100 ns/div) displays transmitter channel 1 output as measured at the antenna port of the Filter/TR switch and highlights the normal symmetric waveform output. DSO channel 2 (10 V/div) (with the T mark indicating the DSO trigger point) displays the PA 7 module output into a 50 Ω load. The marked asymmetry and restricted amplitude of this waveform is due primarily to a malfunctioning power transistor.

the PA modules of this transmitter chassis. Displayed is the initial and final measured amplitudes of each channel's PA module output driven into the SAPR test equipment load. It was found that six out of the ten PA modules of this transmitter chassis

Channel	**Initial Amplitude** [V]	**Transistors Replaced**	**Final Amplitude** [V]
1	25	2	91
2		1	89
3	90	-	90
4		-	104
5	30	1	88
6		1	88
7	14	1	89
8		1	87
9	88	-	87
10	99	-	100

Table 2.8: PA module characteristics of transmitter three pre- and post-maintenance. All measurements has the PA driving the Tx monitor out 50 Ω (20:1 attenuation) load of the SAPR test transmitter rack, except channel seven which is driving the specially constructed 50 Ω load. All Amplitude values are Peak-to-peak (Pk-to-Pk). The number of power transistors replaced in each PA module is also indicated.

had faulty power transistors (power MOSFETs). A test to isolate the set of poorly functioning transistors on the PCB has been devised [*Woithe & Grant*, 1999] which can be applied before individual components are removed from their mounts for specific component testing. A different implementation of these transistors may improve this situation, in particular, the use of heat sinks on this module PCB would be a more thorough implementation of this transistor arrangement.

The application of maintenance techniques to the primary transmitter channel components of Phase Control, Filter/TR and Power Amplifier modules in turn has addressed all known power and phasing problems of the MF transmission system to date. This return to radar specification is confirmed by the parameters displayed in Table 2.9. This table shows the post maintenance amplitude and phase values for a vertically directed beam and should be compared with the pre-maintenance values displayed in Table 2.3 for a measure of the level of improvement obtained. Examining

the data for each transmitter chassis it is apparent that all channels now show a more consistent amplitude behaviour, with adjacent channel amplitude deviations markedly reduced to those encountered in the pre-maintenance case. The temporal behaviour of the reference channel is again present, with its small amplitude variations (± 0.4 V) indicative of a normally functioning channel. The amplitude behaviour across transmitters is difficult to compare in absolute terms because of the remaining variation in the external CRO trigger circuit used to obtain the measurements. Expected behaviour is that transmitter one and two should be identical and that transmitter three displays its effective increase in power. Transmitter three's external CRO trigger occurred at approximately two-thirds peak amplitude of the transmitted waveform and if this is factored in the results, the expected amplitude levels are obtained for the 50 kW transmitter. In terms of the phasing characteristics, twenty-seven out of the thirty channels are within phase specification of $\pm 6^{\circ}$, with two channels being only one nanosecond outside specification and another channel two nanoseconds outside. It is assumed that component tolerances within the system have more of an effect on these three channels relative phase behaviour lying just outside the nominal specification than do the presence of any further concealed faults.

Transmitter	**Channel**	**Amplitude** [Volts]	**Amplitude Reference** [Volts]	**Phase** [ns]	**Relative Phase Behaviour** ch lag/lead ref ch
1	1	24.8	-	-	-
	2	24.6	24.6	4	2 lags REF
	3	22.2	25.0	2	3 leads REF
	4	25.8	25.0	negligible	
	5	23.2	24.8	4	5 leads REF
	6	22.8	24.4	3	6 leads REF
	7	25.8	24.4	3	7 leads REF
	8	23.0	24.8	negligible	
	9	24.8	24.8	7	9 lags REF
	10	24.8	26.4	negligible	
2	1	29.4	-	-	-
	2	29.2	29.4	5	2 leads REF
	3	29.6	29.4	5	3 lags REF
	4	31.4	29.8	5	4 leads REF
	5	30.0	29.2	3	5 leads REF
	6	29.0	29.4	negligible	6 lags REF
	7	31.0	29.4	8	7 leads REF
	8	29.6	30.2	7	8 leads REF
	9	29.6	29.4	4	9 leads REF
	10	29.8	29.8	negligible	10 leads REF
3	1	25.0	-	-	-
	2	25.2	25.0	4	2 lags REF
	3	25.0	25.2	negligible	
	4	25.6	25.2	negligible	
	5	24.4	25.2	4	5 lags REF
	6	23.2	24.4	3	6 lags REF
	7	25.0	24.4	3	7 leads REF
	8	23.8	25.0	2	8 lags REF
	9	22.4	24.8	1	9 leads REF
	10	29.8	24.8	negligible	

Table 2.9: Post-maintenance channel amplitude and phase using a vertically directed transmit beam. The amplitude values display a consistency between channels not evident in the pre-maintenance case (note channel 6 and 9 of Tx-3 need further power optimisation). Phase is within $\pm 6^{\circ}$ for most channels. The three channels exhibiting phase values just outside specification are thought to be the result of minor component tolerance variations and not due to continuing core PC module faults.

The sources of the power and phasing problems uncovered and rectified covered a wide area of transmitter hardware. Faults of some type were addressed in all primary modules of a transmitter channel. The Filter/TR switch module of transmitter one exhibited de-tuned filters while over-stressed chokes were found on all transmitters, with transmitter two being severely affected. The power amplifiers of transmitter three were heavily affected by power transistor failure which is apparently indicative of the 5.0 kW design. Minor choke problems were also encountered on this module. However most channel faults were traced to the PC modules. These critical modules suffered many component problems across the thirty transmitter channels. Solutions to the problems have dramatically increased reliable operation. The documentation of the problems encountered so-far should go some way to effective management of this system component's behaviour in the future. In fact, because of the reliance of the overall system operation on the health of the phase control modules, a future maintenance approach may incorporate the substitution of spare phase control modules, in place of temporarily malfunctioning types. This would allow testing of a revised component design while maintaining a fully operational transmitter chassis.

As part of the research conducted a maintenance approach to the system has been established that now effectively deals with many routine operational issues of the radar system. Specific maintenance techniques have been documented for MF Doppler radar users which simplify the routine maintenance and reduce the total maintenance time expended (i.e. *Woithe & Grant* [1999]). The establishment of a standard Phase Control module calibration procedure has increased the operational reliability of the transmitter system whilst providing a more accurate picture of true, fault free PC module performance. This new benchmark in performance reduces time expended on future fault isolation. As a result of the maintenance described above, the radar has experience a dramatic reduction in logged problems post maintenance.

2.3.2 Extension to three transmitters: problems & solutions

Further limiting the radar's function were problems associated with its ability to beam steer. This applied initially to the coupled 25 kW transmitters and later with the inclusion of the 50 kW transmitter. The radar was often unable to direct a beam bore sight at small off-zenith angles and regularly had difficulty attaining medium to large off-zenith directions. This severely limited the proposed meteor experiments earmarked for trial as well as implementation of regular wind estimates derived via the Doppler beam swinging (DBS) technique [*Woodman & Guillen*, 1974]. The research flexibility afforded by beam-steering dictated that this function be restored to the radar's feature set in the immediate future.

Up to this point routine radar operation was carried out using the two 25 kW transmitters. The integration of the third 50 kW transmitter into this system was necessary to increase received echo power and thus increase the height coverage of routine results. However, before an effort was initiated to integrate the third transmitter into the system it was thought prudent to eliminate any persisting faults in the joint operation of the existing coupled 25 kW transmitters. Because both 25 kW transmitters could phase zero effectively, it appeared that communication was functioning between the RDAS and transmitter. This suggested a further fault in the transmitter chassis that was limiting normal beam-steering operation. It was surmised that beam-steering operation was hampered by a) the PC module not receiving the correct beam phasing pulses or b) the pulse not being properly read due to noise present in pulse message. As discussed previously, the first phasing function initiated by the radar controller before an acquisition is the phase zero process which is applied to obtain a consistent phase output of all channels (i.e. a phase calibration). All faults in this function, across the three transmitter chassis, had been addressed by the procedures outlined in the previous section and all channels were now performing as expected in this respect. A second phasing function is required if the beam bore sight is to be directed off-zenith,

where immediately before acquisition occurs each phase control module steps its channel's output the required phase offset. It was this second function that could not be adequately completed in one of the 25 kW transmitters. The problem was traced to the output section of the tri-state buffer on one PC module which was responsible for setting six phase control bits (in decreasing order of significance P0, R1, R0, D2, D1 and D0) that facilitated this phase shifting of the modules. A blob of solder was discovered crossing control lines D2 and D0 between the tri-state buffer output and the rear 32-pin (edge) connector of the PC module. Once removed, the expected phase shifting function was restored to the system.

With the dual 25 kW transmitter system fully-operational and all known faults corrected in the third 50 kW chassis, these separate transmitter chassis could be integrated as originally designed. The linking of the three transmitter chassis however resulted in a range of abnormal behaviour in the system's initialization sequences and in the operation of previously repaired modules. This suggested faults in hitherto unexamined components of the 50 kW transmitter. With attention directed toward the third transmitter's control modules, further evidence of undocumented modifications to transmitter system modules was revealed, in this case concerning the transmitter control interface and its partner board. This module interfaces the radar controller to each ten channel transmitter sub-system. It was found that the third transmitter's complement of boards did not conform to that described in the system technical documentation. The apparent modifications were documented and its operation was tested. During these tests it was discovered that the colour coded wire connections at the rear of the Tx Control Interface module board were faulty. Multiple connections displayed a lack of electrical contact that appears to be responsible for the intermittent nature of the observed faults. It appears that an incorrect diameter wire has been used or the installation tool used was malfunctioning for these connections. The faulty connections were re-conditioned with larger diameter wire and normal behaviour restored to the linked transmitter chassis.

The isolation and repair of these faults that had previously limited the system's ability to set the phasing of each transmitter channel now allowed the consistent transmission of increased power in off-zenith beams. This result is illustrated in Table 2.10 which displays the amplitude and phase behaviour of all transmitter channels of a beam directed eastward at 20° off-zenith. Each transmitter chassis fed consecutive antenna groups of adjacent rows of the array. This means that the phase steps applied to each channel of a single transmitter are replicated across all transmitters if the desired beam angle is to be obtained.

On average these values are ±12 ns from their expected values. The increase in error for this off-zenith directed beam compared to ±6 ns error for a vertically directed beam arises because two separate phasing operations have been performed in the former case and each single phasing operation has an error of ±6 ns. Minor phase discrepancies of individual channels are again attributed to variations in component tolerances and are not interpreted as indications of continuing channel faults. Further evidence of the increase in transmitted power from the application of the three transmitter chassis was confirmed by the observation of a 4 hop signal for the first time (see section 1.1 for ionospheric layer information and sections 2.3.8 and 5.1.1 for a definition of multi-hop modes and how such modes are supported).

Transmitter	**Channel**	**Amplitude** [Volts]	**Amplitude Reference** [Volts]	**Phase** [ns]	**Relative Phase Behaviour** ch lag/lead ref ch
1	1	24.2	-	-	-
	2	25.4	24.2	100	2 lags REF
	3	22.2	24.4	210	3 lags REF
	4	25.4	24.2	194	4 leads REF
	5	23.0	24.0	106	5 leads REF
	6	23.0	24.0	12	6 lags REF
	7	26.0	24.2	100	7 lags REF
	8	23.4	24.0	218	8 lags REF
	9	25.6	24.2	182	9 leads REF
	10	24.0	24.2	88	10 leads REF
2	1	29.6	-	-	-
	2	28.8	29.6	96	2 lags REF
	3	29.6	29.2	218	3 lags REF
	4	31.2	29.6	196	4 leads REF
	5	28.8	29.2	92	5 leads REF
	6	28.8	29.4	30	6 lags REF
	7	30.6	29.2	110	7 lags REF
	8	29.4	29.4	224	8 lags REF
	9	29.4	29.6	176	9 leads REF
	10	29.6	29.2	80	10 leads REF
3	1	30.0	-	-	-
	2	30.4	30.0	116	2 lags REF
	3	29.4	30.4	222	3 lags REF
	4	31.0	30.0	188	4 leads REF
	5	29.8	30.0	96	5 leads REF
	6	28.4	30.0	36	6 lags REF
	7	29.8	30.0	122	7 lags REF
	8	30.2	30.0	232	8 lags REF
	9	29.0	30.0	162	9 leads REF
	10	36.0	30.4	68	10 leads REF

Table 2.10: Post maintenance transmitter channel amplitude and phase using a beam directed east, 20° off-zenith.

2.3.3 Transmitter pulse leakage problem & solution

With the third transmitter fully integrated into the system a period of preliminary atmospheric observation was undertaken to verify the new configuration. It was during these preliminary observations that it became apparent that transmitter three was exhibiting non-standard behaviour. This took the form of a low frequency signal overlaying expected atmospheric echo and was present in all receivers connected to the 50 kW transmitter chassis to some degree. In fact earlier trials with this chassis had also produced a similar problem. This contamination of the atmospheric signal has

a significant impact on the time-series recorded and on any parameters derived from it. A software approach, via filtering algorithms, was determined to be inadequate as a solution in this instance because of the level of contamination and its suspected inherent hardware nature. This section describes the isolation and repair of this fault.

This extraneous signal could be identified via external CRO monitoring or through the recored time-series to span ranges from 20 to 70 km, demonstrating a gradually increasing intensity up to ∼46 km and trailing off thereafter. While all channels of transmitter three were affected, some were more severely affected than others. The signal was present with transmission into dummy loads, thus excluding any atmospheric phenomena as a possible cause. The following figures illustrate the extent of the problem. Figure 2.10 displays the output from two distinct channels. Both signals displayed in this figure are from a feed taken inside the Filter/TR switch module when driving a dummy load and are representative of signals transmitted into individual or groups of antennas. The waveform labelled channel 1 (upper waveform) displays the output of a normal channel (i.e. Tx-1, Filter/TR-3). This RF burst is approximately 150 μs in extent and has three distinct regions. The first region is a low amplitude varying signal, beginning at the trigger mark (T) and extending approximately 5 to 10 μs. This is followed by the main Gaussian shaped pulse region of approximately 35 to 40 μs whose amplitude envelope extends off the vertical scale. The third region follows the main Gaussian section and extends for 100 to 110 μs. This region is characterised by a decaying amplitude envelope with an initial amplitude of approximately 2 V. The waveform labelled channel 2 (lower waveform) displays the abnormal output from a channel severely affected by the observed low frequency signal. A similar overall character to the first waveform is apparent with some notable differences. The third region shows a much more defined signal with an amplitude envelope that is damped at a reduced rate from an initial value of ∼4 V.

To ascertain the extent of the RF burst signal applied to the transmitter and hence the expected duration of transmitter output, the RF burst signal from the RDAS was viewed in relation to the abnormal Filter/TR switch output. This comparison is

illustrated in Figure 2.11. The RF burst signal (upper waveform) can be seen to extend ∼150 μs and is typically measured at other points in circuit to be 22 V. This compares to the nominally specified 100 μs, 30 V peak-to-peak burst.

Through the interchange of normal and abnormal modules within the system the source of this higher power trailing breakthrough was traced to the PA modules. The PA modules were difficult to test as housed in their channel positions within the transmitter chassis because of the limited physical access to them. Thus more extensive testing was conducted using the SAPR radar system mentioned previously which contained a lower power version of the PA module being tested. Figures 2.12 and 2.13 display the normal output from the 2.5 kW PA module of the SAPR 1.94 MHz radar and the abnormal 5.0 kW PA module of channel four of transmitter three respectively. Each figure contains two waveforms measured at different locations in the PA module tested. The upper waveform in each figure displays the output as taken near the reflected power detector of the PA circuit and the lower waveform shows the output at the 50 Ω dummy load. Figure 2.12 represents the expected output from a PA module. Both waveforms of this figure display a fundamental of the transmit frequency in the presence of four higher-order odd harmonics. These higher-order odd harmonics are removed or at least significantly reduced in the filter section of the Filter/TR switch module before transmission.

In comparison, Figure 2.13 shows output from a channel of transmitter three that is severely affected by the extraneous signal. As both figures are identically scaled, the increased power output of the 5.0 kW PA module compared to the 2.5 kW module is apparent. More importantly, the waveforms in this figure exhibit a lack of high order odd harmonics and appear to have only the third and fifth present. This may not be sufficiently filtered by the action of the Filter/TR switch module.

Because this behaviour is pronounced within the 5.0 kW PA modules and there is some variation in the level of this behaviour across the 5.0 kW boards, its cause may lie in the particular implementation of the extra transistors added to the nominal 2.5 kW design in order to boost output power. The physical placement on the boards and

their possible out-of-specification implementation due to the absence of appropriate heat sinking may hamper their performance.

In order to contain this behaviour of the 5.0 kW PA module a number of solutions were short listed for examination. These were;

1. Shorten RF burst signal from the RDAS to 75 - 100 μs.

2. Improve isolation of receivers from transmitted pulse via additional diodes on Filter/TR switch module to clamp transmitter breakthrough.

3. Clip the RF burst inside the transmitter chassis to exclude the decaying tail.

The first approach would limit the degree of breakthrough transmitted by shorting the duration of the RF burst. This RF burst was measured to be of longer duration and lower amplitude than that specified and appears to be able to accommodate such a reduction in duration without significantly affecting the important Gaussian region of the transmitted waveform. This would curtail the amount of trailing region transmitted in the abnormal case to a level better suited for the action of the filter and diode section of the Filter/TR switch. Difficulties with this proposition were that little technical documentation of the RDAS was available at the time of maintenance and the reduction in RF burst duration may have unpredictable ramifications within both RDAS and transmitter. These disadvantages were sufficient to exclude this particular approach from further scrutiny.

The addition of extra diode sets onto the transmit/receive circuit section of the Filter/TR switch module, in order to better isolate the receivers from the waveform transmitted, was a cost effective solution worthy of trial. An increasing number of diode sets were added to the those already in place. While some reduction in the level of break-through signal was achieved, the overall results were inconsistent and indicated that this approach would not provide the desired level of extraneous signal reduction.

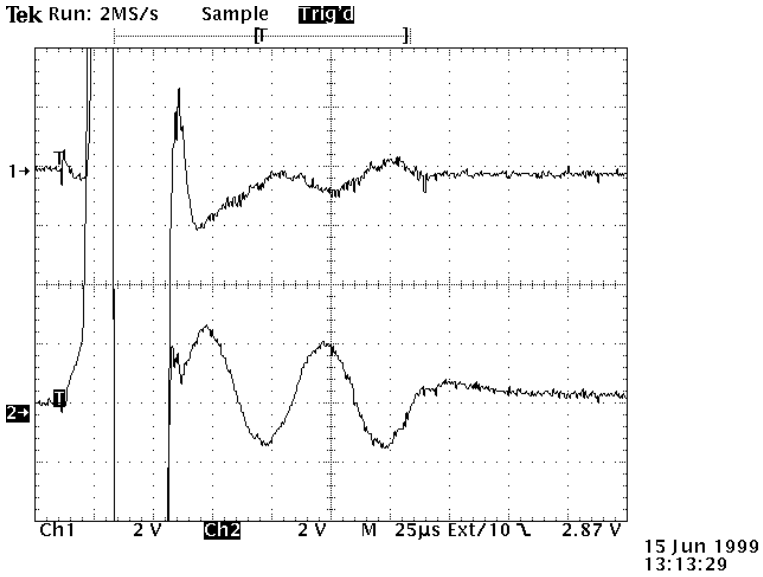

Figure 2.10: Normal and abnormal Filter/TR switch module output. The Filter/TR switch module signal displayed is measured near the output section of the module as it drives a matched dummy load. Digital storage oscilloscope channel one (2 V/div, 25 μs/div) (upper waveform) shows expected transmitter channel output (Tx-1, Filter/TR-3) and DSO channel two (2 V/div, 25 μs/div) (lower waveform) displays an abnormal transmitter channel output (Tx-3, Filter/TR-4) that exhibits a more pronounced trailing 100-110 μs region that may be responsible for the low frequency signal observed in the recorded in time-series.

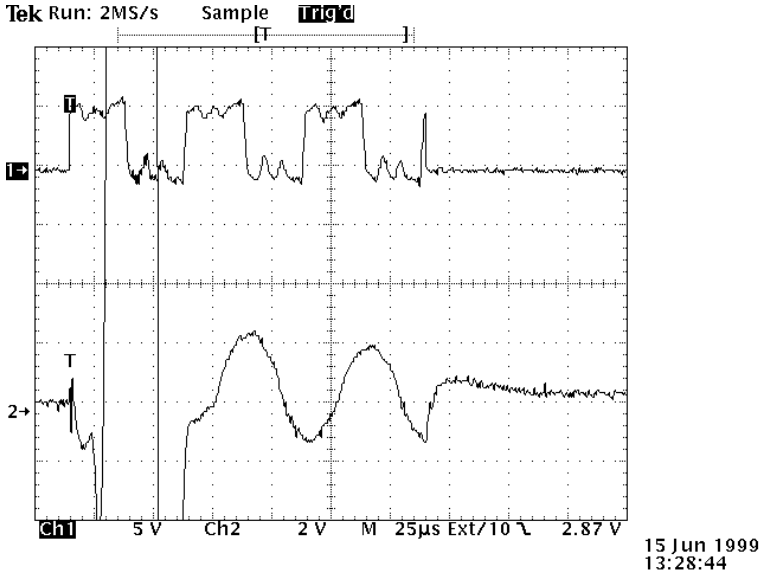

Figure 2.11: RDAS RF burst and abnormal Filter/TR switch module output. DSO channel one (upper waveform) displays the zero degree reference RF burst from the RDAS as presented to the transmitter and channel two (lower waveform) displays the abnormal signal of an affected transmitter channel as per the previous figure. The RF burst indicates how long the transmitter is operative for and thus the extent of high amplitude quasi-sinusoidal third region signal included for an abnormal channel.

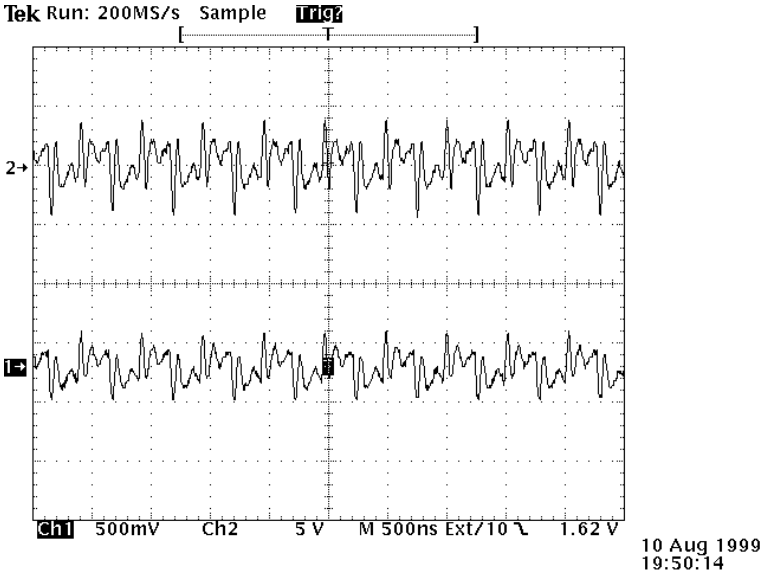

Figure 2.12: 2.5 kW Power amplifier module output: Standard behaviour. DSO Channel one (500 mV/div, 500 ns/div) (lower waveform) displays the output of a standard 2.5 kW PA module (SAPR) as driven into a matched 50 Ω dummy load. Channel two (5 V/div, 500 ns) (upper waveform) displays the output as viewed near the reflected power detector circuit section of the PA module. Note the high frequency (higher-order harmonic) content of the waveforms, which is removed subsequently by the action of the filter section of the Filter/TR switch module.

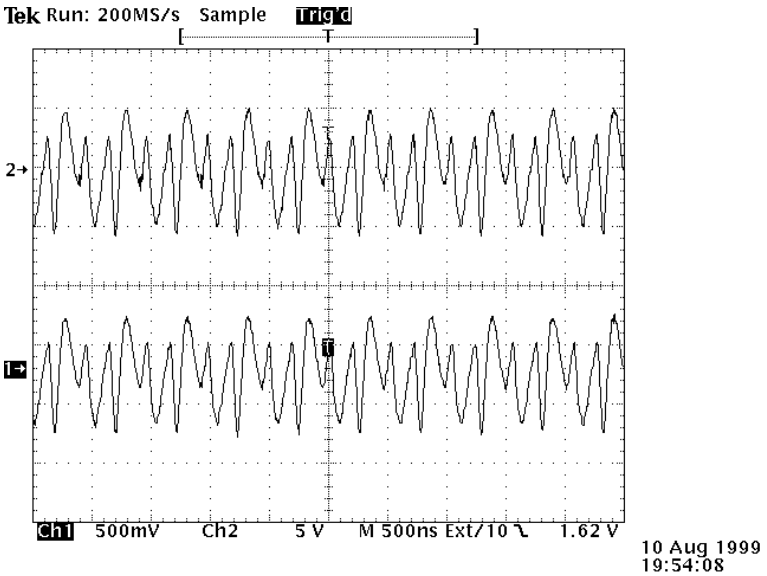

Figure 2.13: 5.0 kW Power amplifier module output: Abnormal behaviour. In a similar format to the preceding figure, the higher power of the 5.0 kW module is apparent, as is the presence of a low order harmonic added to the fundamental. This extra third order harmonic may not be adequately removed during the subsequent filtering provide by the Filter/TR switch module.

An alternative to curtailing the RF burst at its source was to limit it at the transmitter. A design for a circuit that could be retro-fitted to the third transmitter chassis

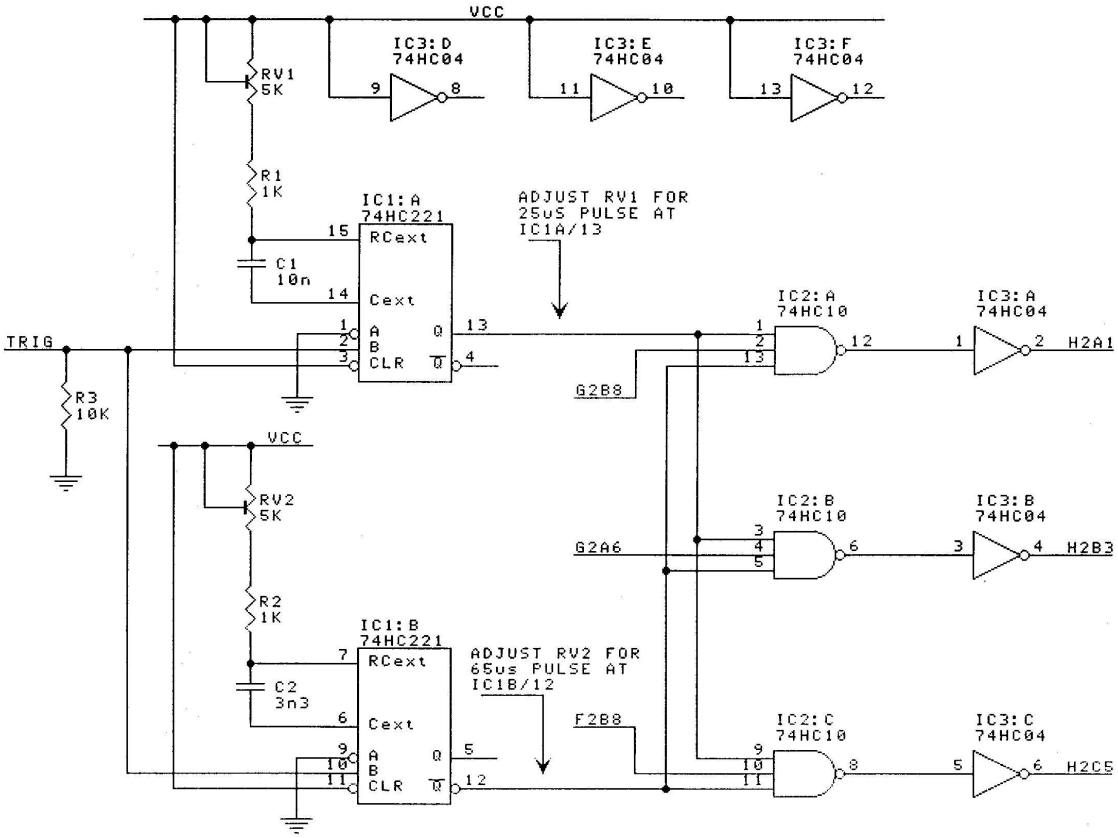

Figure 2.14: Circuit schematic of the clipper daughterboard [*Woithe*, 2000*b*].

(or Tx-1, Tx-2) to achieve this aim was produced [*Woithe*, 2000*b*, private communication]. A daughterboard that could be attached to the Tx Control Interface module was to contain this additional circuit. This facilitated easy fitting to the existing module while retaining the module's original function if need be. When the module is placed on an extender card for testing purposes, access to all the daughterboard's control points would be available. This enabled the on-site selection of the pre- and post-pulse clipping points. The circuit design for this daughterboard is illustrated in Figure 2.14 and interfaces with the Tx Control Interface. The PCB layout and overlay designs are displayed in Figure C.1 of Appendix C. At the time of writing the third transmitter was being utilised for research at a remote site and thus precluded the final implementation and testing of this circuit.

2.3.4 Miscellaneous transmitter problem & solution

Over the maintenance period applied to the MF radar system there were a number of other minor faults detected that affected some not insignificant aspect of radar operation. The details of one such problem and its solution is outlined here due to its pertinence to previously described transmitter faults.

Each transmitter has three rotary fans housed near the bottom of the transmitter chassis for internal cooling purposes. If one or more of these fans in each chassis malfunctions, that transmitter is automatically shut down as a precautionary measure. Because of their essential role in normal transmitter operation and their effect on overall radar operation if a fault condition exists, the behaviour of the fan system must be maintained at all times. It was found that transmitter three had two non-functioning fans. The fan types had a mean lifetime of $\gtrsim$ 50,000 hrs and this particular transmitter had seen little continual operation in its lifetime. Aside from this it was discovered that no fan speed monitor PCB had been implemented for this transmitter chassis and thus offered no feedback on the fan status anyway. Replacement rotary fans and a system fan monitor PCB were installed and tested in the third transmitter. Whether this fan failure had at some point contributed to the extensive failure of the PA module transistors amongst other failures in transmitter three is difficult to ascertain.

2.3.5 Receiver problems & solutions

As most radar operational irregularities had occurred within the transmitter system less maintenance activity had been direct toward the Radar Data Acquisition System (RDAS) component. This RDAS chassis housed sixteen individual receivers amongst other components and a brief investigation of some aspects of its operation was conducted throughout transmitter system maintenance.

A primary concern of the receiver system throughout maintenance procedures and

normal atmospheric observation was the consistent behaviour of each receiver channel. In terms of the maintenance conducted on the transmitter system it is important to isolate any poorly performing receiver channel as a source of under-performing radar channel, so valuable maintenance time is directed toward the fault source rather than fully-functioning channel components. Furthermore, an under-performing receiver channel during data collection can significantly affect the quality of data and the parameters derived from it. This situation is compounded if data from a number of different receivers, with different performance capabilities, are used for parameter reduction, as is the case in cross correlation calculations in FCA analysis and angle-of-arrival determination required for meteor observations.

To better establish current receiver function a signal was injected into the RF input of a receiver and the output measured at its intermediate frequency port. The gain of each receiver can be controlled by the selection of a voltage on a control line to each receiver and was set at 0 dB (indicated by a nominal 8.0 V control signal applied to each channel). During normal atmospheric observations a selected receiver gain of 0 dB often optimises the dynamic range of the receivers for normal daytime atmospheric signal without extensive saturation being evident from intense regions of ionization. Table 2.11 displays the results of this study. This table illustrates a significant difference in gain characteristics of the two receiver types in the system. As mentioned previously, receiver channels eleven to sixteen incorporate a revised receiver design resulting in a physically smaller module footprint. As currently calibrated, receivers eleven to sixteen have a 10 mV reduced output when compared to the original receivers. Examining each receiver type separately, it appears that receiver five is markedly down on signal output when compared to adjacent original receivers and receiver sixteen appears to be malfunctioning in its output behaviour when compared to the receivers of revised design type. These have been noted for fault rectification.

Extended atmospheric observations appear to corroborate this measured discrepancy in receiver gain of the two receiver types. It is sometimes observed that daytime

Channel	**Input** [μV]	**Intermediate Frequency Output** [mV]	**Gain control Voltage** [V]
1	100	16.5	8.00
2	100	16.0	8.00
3	100	18.5	8.00
4	100	15.5	8.00
5	100	11.0	7.98
6	100	15.0	7.98
7	100	16.0	7.99
8	100	15.0	7.99
9	100	14.5	7.99
10	-	-	-
11	100	5.0	7.99
12	100	6.5	7.99
13	100	6.5	8.00
14	100	5.0	7.99
15	100	5.0	7.97
16	100	noise	7.98
16	160	just a signal	7.98
16	200	5.0	7.98

Table 2.11: Receiver channel gain characteristics. This table displays the channel-by-channel receiver gain behaviour for a gain configuration typical of that applied for routine atmospheric data collection. Individual receiver gain is set at 0 dB and Automatic Gain Control (AGC) is not active. Aside from the specific receiver problems exhibited by receiver five and sixteen, the different response of the two receiver types is evident.

E-region echo will saturate the older style receivers (1-10), while the newer style remain unaffected (11-16) for a gain setting of 0 dB. This is a noteworthy consequence of the inconsistent receiver gain behaviour. A primary aim within any receiving system is to fully utilise a receivers dynamic range without inducing saturation (either analogue or digital). Currently this is not being achieved at all times over all receivers partly because of this measured receiver gain discrepancy. It should be remembered at this point that achieving a consistent signal level from most RF receivers is achieved in part by an implementation of an automatic gain control (AGC) function. This facility is incorporated into the MF radar system but has been under utilised in general radar

operation because of poor performance. This centres around the software AGC algorithm that often optimises the gain for one height resulting in poor coverage at other heights. Assuming the AGC operation can be further optimised in software we will describe one approach to achieving a more consistent signal level for most atmospheric conditions.

If the inherent gain of the early style receivers 1 to 10 is reduced to a level at or below that of the newer style receivers and the newer style receivers are maintained at or marginally reduced to match this new inherent gain level, this will eliminate any receiver saturating under normal atmospheric observational conditions at the expense of a temporarily reduced recorded signal level. To then optimise the receiver output from this point, it is suggested that the AGC be tested and re-introduced during all routine operations. When operating as intended, AGC will best optimise the dynamic range of matched receivers by auto-adjusting the gain control voltage on the next acquisition according to the saturation experienced in the previous acquisition.

Assuming that AGC is re-introduced it is sagacious to investigate receiver behaviour over various gain settings. The receiver gain may be selected in software over the range 0 to 60 dB if required. The receiver output for a nominal gain setting of 60 dB is illustrated in Table 2.12 for the original receiver types. There appears to

Channel	**Input** [μV]	**Output** [mV]	**No input** [mV]	**SNR** [dB]
1	1	150	50	9·5
2	1	140	40	10·8
3	1	160	40	12·0
4	1	155	50	9·8
5	1	120	40	9·5
6	1	130	50	8·3
7	1	140	50	8·9
8	1	125	45	8·9
9	1	120	45	8·5
10	1	160	50	10·1

Table 2.12: Receiver channel SNR characteristics at a nominal gain setting of 60 dB. All receivers are of original design type. Notable SNR variations are apparent.

be a significant variation in the SNR of adjacent receiver channels with a 3.7 dB difference between lowest and highest channel output across all functioning receivers. If AGC was active and commonly required gain adjustments over the 0 to 60 dB range it is important that the receivers have consistent output for each nominal gain step when compared to neighbouring receivers. Consistent output of these receivers may be attained through adjustment of specific circuit components. Measurements at various intermediate gain settings will indicate whether receiver function scales linearly after these adjustments.

Even if re-implementing AGC is not possible the benefits of adjusting all receiver's gain characteristics to best encompass commonly experienced atmospheric behaviour without saturation is deemed worthwhile as this would extend the number and effectiveness of the receivers for observation while avoiding the difficult post acquisition task of removing heavy saturation from radar time series. Similarly, aiming for a uniform response of all receivers under varied gain demands will benefit subsequent data reduction.

2.3.6 Data transfer problem & solution

Having isolated and rectified many faults within the transmitter hardware, attention was directed to other areas of the system. One such area encompassed the transfer of large data sets between the radar controller and data analysis computer under specific load conditions. The renewed hardware capability had widened interest in applying the radar system to a varied range of experiments including new approaches to established research interests. Two of these interests were re-creating the phase path measurements of ionospheric irregularities using a spaced antenna arrangement (e.g. *Vincent* [1969]; *Vincent* [1972]; *Schrader & Fraser* [1975]; *Robinson & Dyson* [1975]; *Ahmed* [1977]; *Ball* [1981]) and the observation of meteors. One common requirement of both these types of experiments was the accumulation of larger sized data sets per acquisition than was routinely the case. The ionospheric irregularity experiments typically required four spaced receivers collecting an extended data set, while meteor

observations required at least five receivers (see section 6.3.2) with an extended height range compared to that previously used as well as moderate temporal record lengths. Time series collected with no coherent integration was considered an advantage in the phase path experiment and a necessity in the meteor experiments primarily because of the known short time scale fluctuations of the intended target. This data demand revealed some weaknesses in the data handling capabilities of the MF radar system.

Specifically, if consecutive datasets are to be accumulated the MF radar must first be able to accumulate the required data set size in memory (both physical (RAM) and virtual (hard disk)) and secondly, at the conclusion of the acquisition, be able to transfer it to the analysis computer before the next data set is required. Maintaining a regular acquisition programme (with limited dead time) is also an important aspect of accurately describing many atmospheric targets of interest. Limitations were apparent in both these aspects of radar operation when applied to non-routine atmospheric observations.

Firstly, the radar controller allocates a memory buffer before acquisition begins, comprising physical and virtual memory up to a maximum size of about 20 MB (i.e. $2 \times$ datasize)[7], in readiness to receive data from the RDAS. Once the size of the memory required exceeded that which could be contained mostly in physical memory, this allocation time became excessive and severely limited the flexibility required for atmospheric observations. Although once allocated it need not be reallocated until there is a change in data set size. The radar controller then reads the 32-bit data output from the RDAS during the acquisition and maintains it in radar controller memory for reduction to 16-bit values. This limits the size of the stored data file to about 10 MB per acquisition.

Secondly, there were limits on data set size, with the size a function of 1) the number of points sampled; 2) the in-phase and quadrature components; 3) the amount of coherent integration; 4) the number of receivers used and 5) the height range sampled. Each of these parameters has a numerical limit, determined by parameters in

[7]Note that sizes exceeding this limit resulted in First In, First Out (FIFO) errors.

the RDAS erasable programmable read-only memory (EPROM), that when exceeded causes acquisition errors to propagate throughout the system. These parameter limits are not documented. This can limit the type of experiment configured. As an example, the total number of samples contained within a single acquisition is determined by a parameter called the pulse counter. This parameter is determined by multiplying the 16-bit number of pulses by the 16-bit number of coherent integrations. This allows a high total number of samples (or radar pulses) provided a significant number of coherent integrations are specified. However some radar applications stipulate no coherent integration of the data, which effectively limits the pulse counter to the number of pulses only. Similar parameter limits in the total number of heights, and no doubt other parameters, begin to have a detrimental effect on the flexible application of the radar in observing atmospheric phenomena. It should also be noted that the limits of these parameters are also determined by the capacity of the FIFO chips used to buffer the digitised receiver output within the RDAS. As such the parameters may be hardware limited. A lack of information on the RDAS composition and function has curtailed progress in this area.

Finally, because the radar controller is singularly tasked to control the transmitting and receiving system it doesn't have any surplus resources for allocation to file management while radar control is initiated. So the data set accumulated in memory must be purged to the analysis computer before the next time series is acquired. This is facilitated by a having the radar and analysis computers connected to the field site LAN which is nominally rated at 10 Mbits/sec. Typical data transfer rates encountered were of the order of 70 kB/sec. This translated to a transfer time of the order of at least two and a half minutes for a 10 MB file with temporal fluctuations of up to four and a half minutes being observed, depending on network load. In many instances of scheduled investigations this would lead to a file transfer time far exceeding the data acquisition time and thus constitute a very inefficient use of radar resources, resulting in unacceptably high temporarily spaced acquisitions. These competing factors were optimised for the data collected and analysed in this thesis but it should be noted that

little variation was ultimately possible in these experimental parameters once derived.

In order to address these concerns a number of approaches were taken while general hardware maintenance progressed. The radar controller computer was an IBM compatible 80486 PC. It was envisaged that an increase in onboard physical RAM would alleviate some concerns such as the time required for virtual memory allocation. However, the age of the PC mainboard limited any significant increase in this area. A complete computer upgrade was thus instituted at this point. This was expected to improve some aspects of the problems outlined, but not all. When reconfigured with this new arrangement of the radar controller PC it was apparent that the particular version of MS-DOS limited the physical RAM addressable to 64 MB. This improved the data headroom available for larger sized data sets, but they were still ultimately limited by the pulse counter and the transfer rate.

To alleviate the slow data transfer times an upgrade to the network between the radar controller and analysis computer was also instituted. Two 100 Mbits network cards were installed to form a dedicated point-to-point network that theoretically facilitated a significant increase in data transfer speeds. Interestingly this did not dramatically decrease the transfer times as envisaged. Extensive testing of this configuration has isolated the cause of this under-performance to the MS client for networks used in the radar controller computer. The architecture of the system currently prevents any significant advance in this area. While this new network card configuration improved some aspects (i.e. transfer speed of 600 kB/s) it did not eliminate data transfer timing as a factor in radar operation. Significant limitations of this system remain and studies of implementing a real-time Linux based system for radar control are underway. A successful implementation of such a system will then no doubt direct the focus of overall system limitations to the capabilities of the RDAS alone.

2.3.7 New hardware

When used primarily as a research tool, great flexibility is demanded of the MF radar system. The requirement of catering to varied research interests has been met for

the most part by the large aperture array and 30/16 channel transmitter/receiver system. In particular, the large aperture array has accommodated these requirements by the transmission and reception on all or partial sections of the array, centering on its ability to generate a high power, narrow beam via a large number of individual antennas. However future projects may require an unforeseen configuration of existing equipment or additional hardware to fulfil their aim. One limitation of this array configuration is that each balun of the main array is limited to voltages of between 300 V and 500 V [*Vandepeer*, 1993]. A requirement for higher transmitted powers and a broad beam generated by a single or small number of antennas would seek an alternative arrangement. Two recent research proposals that sought high power on single or small groups of antennas were an investigation into surface wind measurement utilising scatter from the ocean surface and an inter-comparison of the Time Domain Interferometry (TDI) technique [*Vandepeer & Reid*, 1995] when applied with wide and narrow beam systems [*Berkefeld*, 1996, private communication]. The first proposal would utilise the ground wave mode of propagation while the second would direct radiation vertically by convention. In the first instance a new antenna system would need to be utilised [*Grant*, 1997], or existing antennas modified (e.g. *Parkinson et al.* [1993]), to generate surface directed vertically polarised radiation while the latter proposal would incorporate the use of the superseded 1.98 MHz transmit array. This transmit array, comprising two sets of orthogonal dipoles (and its baluns), has typically handled transmitter powers from 10 kW [*Vandepeer*, 1993] through to 50 kW [*Hocking*, 1981] with typical levels of the order of 25 kW [*Olsson-Steel & Elford*, 1987; *Murphy*, 1990].

Obtaining these higher powers coupled to a single or dual output would require the cascading of the individual power amplifier modules of the transmitter in a previously untried configuration. A convenient way to facilitate this is by using a flexible modern power combining system. The design, construction and evaluation of a suitable power combining system formed part of this thesis' research and is thoroughly described in Chapter 4.

2.3.8 Future work

Throughout the course of the work presented in this section a number of areas relating to the hardware and operation of the MF Doppler radar, that would benefit from future attention, have been identified. Areas identified encompass the final construction and evaluation of the transmitter Tx Control Interface modification, general maintenance practices in terms of scheduling and equipment employed, as well as general operational issues. These areas are addressed in the following section.

2.3.8.1 Transmitter

While the third 50 kW transmitter was successfully integrated into the MF Doppler radar system the performance of its power amplifier modules seriously compromised the data collected in many instances due to the presence of a low frequency extraneous signal. The trial of the retro-fitted RF burst clipping daughterboard is of paramount importance if this system is to be included in routine atmospheric observations. The increase in transmitted power that this third transmitter offers is of significant benefit to the parameter estimation during data reduction and to the range of heights covered.

In terms of the number and type of faults identified in the transmitter system during this study, radar performance is likely to have been compromised during certain atmospheric observations. The inconsistent phasing of the channel output for a vertically directed beam is one such example. It is unclear how long this and the other noted deficiencies existed in this radar system. For this reason it is important that a regular maintenance programme is initiated. This would involve performance evaluation at regular intervals and scheduled servicing to address any issues uncovered. This work can be efficiently divided into transmitter, receiver and antenna array work as it has been done here. This allows better use of labour, time and equipment. Of particular importance is establishing whether the transmitter channel output is as desired via the techniques outlined in section 2.3.1. This goes some way in confirming the

radiation produced by the radar in various beam positions. While this technique temporarily omits the antenna array from the system it offers the prospect of eliminating the transmitting system as a fault source in a poor radiation pattern. Evaluating the *actual* radiation pattern of the radar can be a more involved undertaking and some techniques are mentioned briefly below.

Also evident in the preceding maintenance investigations is the utility of maintaining a complete set of working primary transmitter modules. This is vital in maintaining general radar operation but also greatly assists in module fault finding should it arise. In this situation a comparison of identical transmitter modules, in terms of their general behaviour and component values (e.g. Filter/TR switch module L1, L2 and C3 values), allows a better evaluation of the source of module faults. Further to this point, a PA module extender cards need to be fabricated to allow the examination of faulty PA modules *in situ*. This will obviate the need for utilising the SAPR radar chassis for testing. To ensure consistency of scientific results the procurement and use of spare primary system transmitter modules is warranted given the observed natural attrition of these components to date.

The apparent crosstalk between Filter/TR switch modules is also an area identified for further investigation. It appears that there is a measurable sympathetic signal excited in adjacent Filter/TR switches under certain conditions. This needs to be further quantified. Possible solutions to this may be as simple as terminating all unused ports of the Filter/TR switch module or realising a better shielded cable system that feeds this module. Alternatively, more shielding may be necessary on the actual Filter/TR switch module PCB.

It was originally envisaged that the 2.5 kW PA modules of the two 25 kW transmitter chassis be upgraded to the 5.0 kW specification at some juncture [*Reid et al.*, 1995] to achieve 138 kW RMS PEP. The poor performance of the current 5.0 kW PA modules, as detailed in section 2.3.1.3, precludes this design from forming the basis of any replacement. It is suggested that any new PA design seek an alternative arrangement of the power transistors, to incorporate a heat sink of some sort, at the

very least. One advantage of the modular arrangement of the power amplifiers is that a prototype of a new 5.0 kW PA module design may be easily tested in the existing transmitter chassis for an extended period to verify the design approach taken.

The ability to transmit circular polarisation was a design feature of the MF Doppler radar. In terms of night time meteor observations, the ability to transmit right-hand circularly polarised radiation (O-wave) limits the ionospheric absorption experienced (as compared to E-wave or Linear) [*Olsson-Steel & Elford*, 1987]. However, with the de-commissioning of the separate parallel pair of dipoles as the primary transmitter array, only linear radiation has been transmitted to date using the main antenna array. Recently, one transmitter chassis had a reversible hardware modification to its PC modules to enable the transmission of circularly polarised radiation on a suitable antenna system. Options exist to carry this design over to the other transmitter chassis or develop a different implementation involving an altered patching of antenna systems and software modifications to obtain a circular polarisation and beam-steering facility. The inherent flexibility of the latter option is attractive, while the former design is simple and effective for vertically directed beams. It appears that the best solution will perhaps be dictated by the possible applications of circularly polarised radiation.

2.3.8.2 Receiver

In terms of the receiving system, an effort should be made at establishing uniform receiver behaviour with a primary consideration being each devices inherent gain structure. The testing and evaluation of new software AGC algorithms will determine whether this function can be effectively restored as a feature of the system and its suitability for application to routine observations.

Most radars specified lifetime encompasses demands for increased flexibility in terms of its hardware and/or software at some stage, and this is particularly true of research radars like the MF Doppler radar described here. Fortunately the core design of this radar is well suited for future upgrades primarily because of its limited hardware components and the modularised arrangement. However, as has been indicated in the

previous sections, current hardware and software limits have been experienced. Of particular interest is the limitation of the basic radar parameters such as the number of heights and points sampled that are determined by both hardware and software constraints. Most of these limits are traced to the inherent capacity of the RDAS. A detailed electronic investigation of this receiving chassis will ascertain the memory capacity of specific components and thus firmly establish the current limits while highlighting the specific components for possible replacement at some juncture. This will also establish the possible scope of any future modifications to the radar acquisition software. The transfer rate of acquired data from the radar controller to the analysis computer is also of concern and severely restricts the frequency of time series collected during meteor investigations. Progress in these areas will greatly increase the data throughput and enhance post acquisition analyses.

To select independent receivers, *Reid et al.* [1995] indicate that single independent TR switches which mount on the front of the antenna patchboards could be used. Current operational practice instead allows direct connection of a single nominal 75 Ω dipole to a nominal 50 Ω receiver. This nominal impedance transformation will account for some signal loss at the receiver. Also, if connected, a normal group of three dipoles exhibiting a nominal 25 Ω, will exhibit a similar signal loss at the receiver. In addition to this, the receiver input impedance has been found to deviate significantly from its nominal value and thus may present a more significant transformation mis-match. The connection of a single dipole (or less significantly, a standard dipole group) to a single receiver is an important part of standard system configuration and has been used extensively for the results discussed in later chapters. This provides motivation for a more suitable arrangement to optimise the signal received. One approach would be to establish the standard input impedance characteristics of the receivers and tailor a passive transformer for connection inline between antenna patchboard position and receiver. Different transformations could be obtained if groups of dipoles were to be used for input to a single receiver. This arrangement would place less demand on the receiver's low noise pre-amplifier section and thus ensure better subsequent

amplification. As meteor returns encompass a wide dynamic range signal optimisation, pre-receiver input, may allow structure to be better differentiated from noise and thus increase the hourly meteor count rate. Obviously, this would need to be implemented before receiver gain structure is altered.

The phase stability of the local oscillator that enables the coherent capabilities of the receiving system is vital to minimizing errors in the accumulated data. A simple form of coding the transmitted pulses, available to the current system, is that of phase inversion (alternating the phase of every second pulse by 180°). Theoretically, the original time series can be easily reconstructed in software by reversing this process. Attempts to retrieve the original signal from the phase coded data have failed thus far. The resulting data appears to have a small phase offset, such that an artificial envelope is introduced into the time series. One possible cause of this may be traced to the stability of the local oscillator. As mentioned previously, the in-phase and quadrature components of a detected signal are created via the mixing with the local oscillator derived signals. There must be an orthogonal relationship between these components to prevent errors from being introduced into the resulting signal. Indications of acceptable stability are mentioned by *Brown* [1992], in that it should be 0.01 Hz over the time taken for the transmitted pulse to reach 100 km altitude and return, however in the case of phase coded transmission this time must be over at least two pulses or more generally over at least the propagation time of the coding period. If there exists some drift in the mixing signal, this orthogonal relationship will be destroyed and could possibly result in artificial effects being introduced into the phase inverted data as has been observed. This is an area for immediate attention.

2.3.8.3 Calibration

One task that can only be effectively completed with a fully-functioning transmitter, antenna array and receiving system is that of *calibration*. The term calibration often applies to two distinct operations. Firstly, it may indicate the confirmation of the radars transmitted radiation pattern in the form of a polar diagram (e.g. *From &*

Whitehead [1984]). Secondly, it can encompass any technique applied to a radar system to ascertain a numeric relationship between radar parameters such as the power received, reflection coefficients or back-scatter cross-sections of a target for instance (e.g *Hocking* [1989]). In relation to the MF Doppler radar, both calibration approaches would provide valuable information for any subsequent course of atmospheric sensing. The first approach provides a method by which the actual transmitted radiation pattern can be confirmed, including the effects of the antenna array, rather that relying solely on the measured transmitter output as described previously or on antenna modelling programmes. The second approach primarily allows the comparison of data sets to be made between radars in absolute terms because the target return is meaningfully quantified. Note that in order to maintain the validity of either type of calibration performed, in most cases the complete radar system must be maintained in such a way so as to provide operation consistent with that hardware configuration at the time of calibration. The reduction of transmitted power as a result of malfunctioning PA modules will affect any calibration as will modifications to receiver sensitivity for instance. This highlights the need for scheduled maintenance once calibration is performed.

An example of the first type of calibration that has been directly applied to a MF/HF radar was undertaken by *From & Whitehead* [1984]. The authors point out as justification for a more complete estimation of a radar's capabilities, that although you may have a grasp of the phase behaviour through the transmitter and receiver system[8] the antenna behaviour is also important. In our situation the antenna system includes the extensive network of coaxial cable that are known (see Chapter 3) to have a contributing effect on system phase. In their technique, the ionosphere is used as a reflector and the polar diagram is measured as a function of the off-vertical angles when the radar beam is nearly vertical. This technique assumes that there is only one target at the range chosen. A technique using a ground-based test signal and the ionosphere has also been used [*Lees & Blesing*, 1990], while confirmation of radar polar diagram has also been obtained from meteor targets themselves via examining

[8]Via automated self-tests or phase calibration of the transmitter and receiver hardware.

the properties of head echo types [*Elford et al.*, 1995; *Cervera et al.*, 1997], although this method has less application at MF due to the scarcity of these events.

It should be noted that there are alternate techniques available to significantly higher frequency radars that are difficult to be effectively applied at medium frequencies and lower regions of the HF component of the radio spectrum. For instance calibration by balloon or powered aircraft is expensive and logistically difficult. The presence of near-field corrections demand that the chosen airborne platform typically attain an altitude in excess of 10 km [*From & Whitehead*, 1984]. While capable platforms exist their operational expense is a determining factor. Similarly, calibration via radio-sources such as the cosmic noise background [*Lamy et al.*, 1991] or satellites [*Sato et al.*, 1986] are also commonly used for calibration purposes, but in this case, the very frequencies that provide optimal ionospheric signals for ground based radars are unable to penetrate to satellite altitudes effectively.

Calibration techniques to attain the second approach's goal are many and varied (e.g. *Earl & Ward* [1987]; *Hocking* [1989]; *Solomon et al.* [1998]). Some examples of these are outlined briefly below and include using a noise generator as a replacement for the antenna, multi-hop ionospheric echoes and receiver signal direct injection.

A common method of receiver calibration is where a noise generator's signal is injected in-place of the antennas. This will result in the receiver section outputting a signal level of specified units that can be calibrated against the known input signal. One disadvantage of this particular method is that strictly speaking the receiver is calibrated for those conditions experienced at that time. Variations in the performance of the antenna and feeding system will occur as components age and the local weather environment changes as examples.

A relatively straightforward technique proposed by Hocking is applicable to radars within the MF-HF region of the spectrum and exploits the attenuation of the radar

echo experienced in the ionospheric environment [*Hocking*, 1989]. The technique involves using *multiple hops*[9] of a totally reflected pulse from the ionosphere. Here, a calibration constant κ can be determined from the equation

$$\kappa = \frac{2\sqrt{P_t}\sqrt{P_{2R}}}{zP_{1R}} \tag{2.4}$$

Where P_t is transmitted power, P_{1R} is the received power from the first hop and P_{2R} from the second, z is the height of the reflecting layer. If this is substituted into the equation for the received power for the first hop, $P_{1R} = \kappa^{-2}\overline{R}^2 z^{-2} P_t$ and the reflection coefficient R can be determined.

A more complete solution to the calibration of radars is that of injecting a metered signal into the receivers to calibrate against. Unfortunately this type of approach is hardware orientated and as such is generally incorporated into a radar's original design, although certain implementations may be retro-fitted at a later data with a minimum of difficulty. A typical realisation of this type of radar calibration is described for the backscatter and oblique/vertical incidence sounder that forms part of the frequency management system for the Jindalee over-the-horizon backscatter HF radar [*Earl & Ward*, 1987]. Here, a signal of known strength is continuously injected into the receiver. During spectral analysis, the data is normalized to absolute power levels using the calibrate signal as a reference. Variations on this general theme could be applied to most radars. For instance the signal need not be continuously injected, if receiver operation is relatively stable on the order of data acquisition time scales, but may be part of a self-calibration operation before an acquisition that is scheduled periodically. Note that an injected signal of high stability at the receiver will provide a solid reference under the varying conditions that will affect the antennas and cable system.

[9]For instance the second hop echo is the echo from the ionosphere that returns to the ground, is re-reflected to the ionosphere and finally returns to the receiver.